ORGANOMETALLICS Article
Cite This: Organometallics XXXX, XXX, XXX−XXX
pubs.acs.org/Organometallics

Synthetic and Structural Studies of [FeFe]-Hydrogenase Models Containing a Butterfly Fe/E (E = S, Se, or Te) Cluster Core. Electrocatalytic H_2 Evolution Catalyzed by $[(\mu\text{-SeCH}_2)(\mu\text{-CH}_2\text{NCH}_2\text{Ph})]\text{Fe}_2(\text{CO})_6$

Li-Cheng Song,*[†,‡] Jin-Sen Chen,[†] Guo-Jun Jia,[†] Yong-Zhen Wang,[†] Zheng-Lei Tan,[†] and Yong-Xiang Wang[†]

[†]Department of Chemistry, State Key Laboratory of Elemento-Organic Chemistry, College of Chemistry, Nankai University, Tianjin 300071, China

[‡]Collaborative Innovation Center of Chemical Science and Engineering (Tianjin), Tianjin 300072, China

Supporting Information

ABSTRACT: As models of [FeFe]-H_2 ases, 13 butterfly Fe/E (E = S, Se, or Te) complexes (**1**−**13**) have been prepared by various synthetic methods. Treatment of $[(\mu\text{-SCH}_2)_2\text{CH}_2]\text{Fe}_2(\text{CO})_6$ (**A**) and $[(\mu\text{-SCH}_2)_2\text{CHO}_2\text{CPh}]\text{Fe}_2(\text{CO})_6$ (**B**) with the in situ-generated N-heterocyclic carbenes (NHC) $I_{Me/Mes}$, $I_{Vinyl/Mes}$, I_{Mes}, and I_{Me} gave the corresponding carbene-substituted butterfly [2Fe2S] complexes $[(\mu\text{-SCH}_2)_2\text{CH}_2]\text{Fe}_2(\text{CO})_5(I_{Me/Mes})$ (**1**), $[(\mu\text{-SCH}_2)_2\text{CH}_2]\text{Fe}_2(\text{CO})_5(I_{Vinyl/Mes})$ (**2**), $[(\mu\text{-SCH}_2)_2\text{CHO}_2\text{CPh}]\text{Fe}_2(\text{CO})_5(I_{Mes})$ (**3**), and $[(\mu\text{-SCH}_2)_2\text{CHO}_2\text{CPh}]\text{Fe}_2(\text{CO})_4(I_{Me})_2$ (**4**), respectively. Although the *N*-*p*-methoxyphenyl-substituted 1,2,4-diselenazolidine **C** reacted with $Fe_3(CO)_{12}$ to give the expected butterfly [2Fe2Se] complex $[(\mu\text{-SeCH}_2)_2\text{NC}_6\text{H}_4\text{OMe-}p]\text{Fe}_2(\text{CO})_6$ (**5**) and further reaction of **5** with PPh_3 afforded its PPh_3-substituted derivative $[(\mu\text{-SeCH}_2)_2\text{NC}_6\text{H}_4\text{OMe-}p]\text{Fe}_2(\text{CO})_5(\text{PPh}_3)$ (**6**), the *N*-arylmethyl-substituted 1,2,4-diselenazolidines **D**−**F** reacted with $Fe_3(CO)_{12}$ to give the first butterfly [2Fe1Se1N1C] complexes $[(\mu\text{-SeCH}_2)(\mu\text{-CH}_2\text{NR})]\text{Fe}_2(\text{CO})_6$ (**7**, R = $PhCH_2$; **8**, R = $NC_5H_4CH_2$-*p*; **9**, R = $CpFeC_5H_4CH_2$), unexpectedly. More interestingly, on the basis of synthesizing the first ODTe-bridged butterfly [2Fe2Te] complex $[(\mu\text{-TeCH}_2)_2\text{O}]\text{Fe}_2(\text{CO})_6$ (**10**), the NHC-substituted butterfly [2Fe2Te] complexes $[(\mu\text{-TeCH}_2)_2\text{O}]\text{Fe}_2(\text{CO})_5(\text{L})$ (**11**, L = $I_{Me/Mes}$; **12**, L = I_{Mes}; **13**, L = I_{Me}) were prepared by reactions of complex **10** with the corresponding NHC ligands. In addition, while all of the new complexes **1**−**13** were structurally characterized, complex **7** was found to be a H_2-producing catalyst from benzoic acid and *p*-toluenesulfonic acid under cyclic voltammetry conditions.

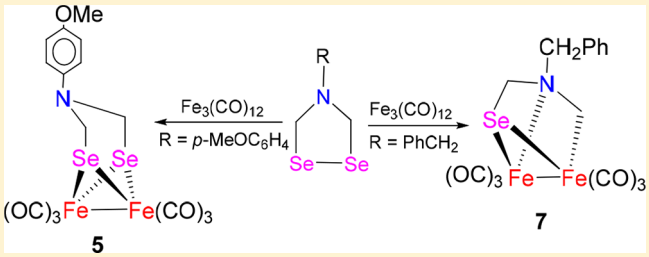

INTRODUCTION

The butterfly Fe/E (E = S, Se, or Te) cluster complexes have received a growing amount of attention in recent years, mainly due to their unique structures and novel properties and particularly the close resemblance to [FeFe]-hydrogenases ([FeFe]-H_2 ases).[1−8] [FeFe]-H_2 ases make up a class of natural enzymes that catalyze the reversible proton reduction to molecular H_2 in a wide variety of microorganisms.[9] X-ray crystallographic,[10−12] FTIR spectroscopic,[13−15] and some other experimental[16,17] studies established that the active site of [FeFe]-H_2 ases (so-called H-cluster)[18] comprises a cubanelike [4Fe4S] cluster that is linked via a cysteine sulfur atom to a butterfly [2Fe2S] cluster in which its two Fe centers are coordinated by three CO ligands, two CN^- ligands, and one bridging azadithiolate (ADT) ligand (Figure 1). On the basis of structural studies regarding the active site of [FeFe]-H_2 ases, a wide variety of butterfly Fe/E (E = S, Se, or Te) cluster complexes as [FeFe]-H_2 ase models have been synthesized and characterized by chemists in bioinorganic and organometallic fields.[19−37] To further develop the synthetic methodology for butterfly Fe/E cluster complexes and to develop the biomimetic chemistry of [FeFe]-H_2 ases, we have prepared four types of new butterfly [2Fe2S], [2Fe2Se], [2Fe1Se1N1C], and [2Fe2Te] cluster core-containing complexes. In

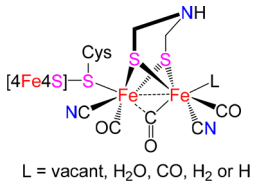

Figure 1. Basic H-cluster structure determined by FTIR and X-ray crystallography.

Received: January 16, 2019

Downloaded via UNIV OF CAMBRIDGE on March 20, 2019 at 15:20:02 (UTC).
See https://pubs.acs.org/sharingguidelines for options on how to legitimately share published articles.

this work, we report their synthesis and structural characterization. In addition, the electrocatalytic H_2 production catalyzed by one of the prepared [2Fe1Se1N1C] cluster core-containing models is also described.

■ RESULTS AND DISCUSSION

Synthesis and Characterization of PDT-Bridged Butterfly [2Fe2S] Complexes Containing One or Two NHC Ligands. N-Heterocyclic carbene (NHC) ligands have been extensively utilized as surrogates for phosphines to prepare the H-cluster mimics of [FeFe]-H_2 ases,[23,24] because NHC ligands have stronger σ-donation with negligible π-accepting ability as well as greater electronic and steric tunability in comparison with those of phosphine ligands.[38−40] On the basis of our previous studies regarding the butterfly [2Fe2S] cluster core-containing model complexes of [FeFe]-H_2 ases,[28−30] we prepared a series of the new PDT (PDT = propanedithiolate)-bridged butterfly [2Fe2S] core and NHC ligand-containing [FeFe]-H_2 ase models. Thus, as shown in Scheme 1, the NHC ligand $I_{Me/Mes}$ ($I_{Me/Mes}$ = 1-methyl-3-mesitylimidazol-2-ylidene)-containing butterfly [2Fe2S] complex (μ-PDT)$Fe_2(CO)_5(I_{Me/Mes})$ (**1**) could be prepared in tetrahydrofuran (THF) at room temperature by CO substitution of parent complex (μ-PDT)$Fe_2(CO)_6$ (**A**) with the in situ-generated $I_{Me/Mes}$ by loss of one molecule of HI from 1-methyl-3-mesitylimidazolium salt $I_{Me/Mes}$·HI under the action of *n*-BuLi.[41] However, different from this, we further found that the NHC ligand 1-vinyl-3-mesitylimidazol-2-ylidene ($I_{Vinyl/Mes}$)-substituted complex (μ-PDT)$Fe_2(CO)_5(I_{Vinyl/Mes})$ (**2**) could be prepared by CO substitution of complex **A** with the unexpectedly generated carbene $I_{Vinyl/Mes}$ by thermal decomposition (β-elimination) of the dicarbene $I^*_{Mes}(CH_2)_2I^*_{Mes}$ initially formed by loss of two molecules of HBr from the ethylene-bridged imidazolium salt $[I^*_{Mes}(CH_2)_2I^*_{Mes}]$·2HBr under the action of *n*-BuLi (Scheme 1).

Scheme 1. Synthesis of NHC-Substituted Butterfly [2Fe2S] Complexes 1 and 2

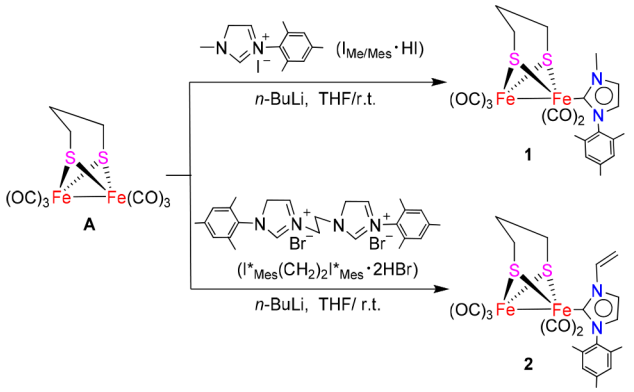

Similarly, the benzoyloxy group-substituted derivative of parent complex **A**, namely complex $[(\mu\text{-}SCH_2)_2CHO_2CPh]Fe_2(CO)_6$ (**B**), was found to react with the in situ-generated NHC ligand I_{Mes} [I_{Mes} = 1,3-bis(mesityl)imidazol-2-ylidene] from 1,3-bis(mesityl)imidazolium salt I_{Mes}·HCl under the action of *n*-BuLi to give the I_{Mes}-monosubstituted complex $[(\mu\text{-}SCH_2)_2CHO_2CPh]Fe_2(CO)_5(I_{Mes})$ (**3**), whereas the NHC ligand I_{Me} [I_{Me} = 1,3-bis(methyl)imidazol-2-ylidene]-disubstituted complex $[\mu\text{-}(SCH_2)_2CHO_2CPh]Fe_2(CO)_4(I_{Me})_2$ (**4**) could be obtained by CO substitution of **B** with the in situ-generated I_{Me} from 1,3-bis(methyl)imidazolium salt I_{Me}·HI under the action of *t*-BuOK in THF at room temperature (Scheme 2).

Scheme 2. Synthesis of NHC-Substituted Butterfly [2Fe2S] Complexes 3 and 4

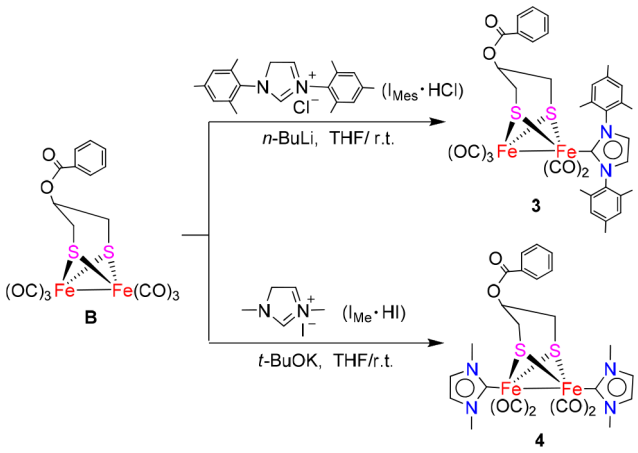

While complexes **1**−**3** are air-stable red solids, complex **4** is an air-sensitive red solid. All complexes **1**−**4** were characterized by elemental analysis and spectroscopy. For example, the IR spectra of **1**−**4** showed three or four absorption bands in the range of 2037−1871 cm^{-1} for their terminal carbonyls, while **3** and **4** showed one additional band at 1709 or 1714 cm^{-1} for their ester carbonyls. The ^1H NMR spectra of **1** and **2** displayed two singlets in the region of 2.10−2.36 ppm for the three CH_3 groups attached to benzene rings in their NHC ligands. In addition, the $^{13}C\{^1H\}$ NMR spectra of **1**−**3** displayed one signal in the range of 189−194 ppm for their carbene C atoms,[31b,42] although the qualified $^{13}C\{^1H\}$ NMR spectrum of **4** could not be obtained because of its instability under the determined conditions.

The molecular structures of complexes **2** and **4** were further confirmed by X-ray crystal diffraction analysis. While their ORTEP views are shown in Figures 2 and 3, the selected bond lengths and angles are listed in Table 1. As shown in Figure 2, complex **2** contains one PDT ligand that is bridged between its two iron atoms and one NHC ligand 1-vinyl-3-mesitylimidazol-2-ylidene located in the apical position of the square-

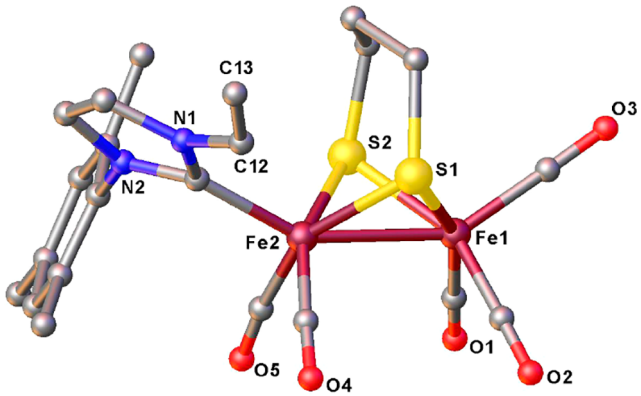

Figure 2. ORTEP view of **2** with 50% probability level ellipsoids. All hydrogen atoms have been omitted for the sake of clarity.

DOI: 10.1021/acs.organomet.9b00022
Organometallics XXXX, XXX, XXX−XXX

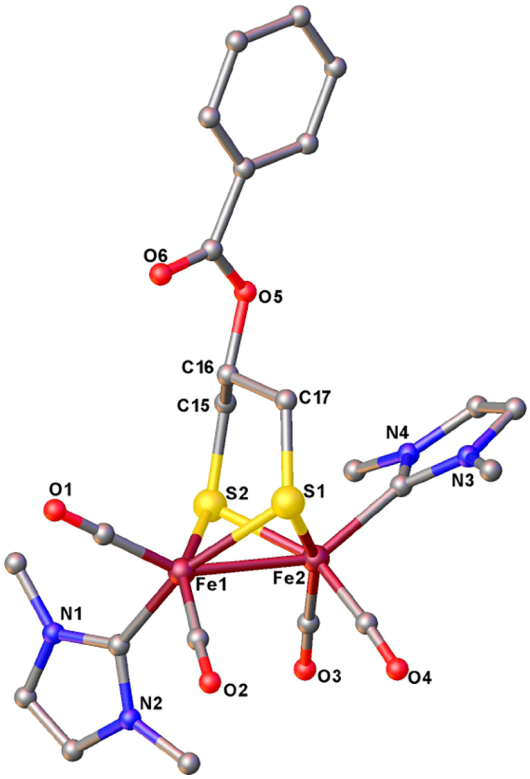

Figure 3. ORTEP view of **4** with 50% probability level ellipsoids. All hydrogen atoms have been omitted for the sake of clarity.

pyramidal Fe(2) atom. The C(12)═C(13) bond length is 1.308 Å, whereas the Fe(1)−Fe(2) bond length is 2.5236 Å, which is very close to that (2.55 Å) of the reduced state of [FeFe]-H_2 ases[12] but much shorter than those (2.60 and 2.62 Å) of the oxidized state of [FeFe]-H_2 ases.[10,11] Figure 3 shows that complex **4** contains one benzoyloxy group-substituted PDT ligand and two NHC 1,3-dimethylimidazol-2-ylidene ligands. The substituted PDT ligand is bridged between two iron atoms to form two fused six-membered rings: one six-membered ring Fe(1)S(1)C(17)C(16)C(15)S(2) with a boat conformation and the other six-membered ring Fe(2)S(1)-C(17)C(16)C(15)S(2) with a chair conformation. The benzoyloxy group is attached to the bridgehead C(16) atom via the common equatorial C(16)−O(5) bond of the two fused six-membered rings, to avoid the strong steric repulsions of the equatorially attached benzoyloxy group with the apically occupied carbonyl at Fe(1) and 1,3-dimethylimidazol-2-ylidene ligand at Fe(2).[4] In addition, the two NHC ligands are unsymmetrically bound to a basal position and an apical position of the square-pyramidal Fe(1) and Fe(2) atoms, respectively.

Synthesis and Characterization of Butterfly [2Fe2Se] and [2Fe1Se1N1C] Cluster Core-Containing Complexes. On the basis of our previous study of the butterfly [2Fe2Se] model complexes,[31−33] we prepared the new azapropanediselenolate (ADSe)-bridged butterfly [2Fe2Se] complexes **5** and **6**. Thus, as shown in Scheme 3, when *N*-*p*-methoxyphenyl group-substituted 1,2,4-diselenazolidine **C**[43] was treated with $Fe_3(CO)_{12}$ in THF at 60 °C, the corresponding N-substituted butterfly [2Fe2Se] core-containing complex [(μ-$SeCH_2)_2NC_6H_4OMe$-*p*]$Fe_2(CO)_6$ (**5**) was obtained via the oxidative addition of the Se−Se bond in diselenazolidine **C** with diiron fragment $Fe_2(CO)_8$ [formed in situ by thermal decomposition of $Fe_3(CO)_{12}$] and subsequent displacement of its two CO ligands.[35] In addition, upon further treatment of **5** with PPh_3 in the presence of decarbonylating agent $Me_3NO\cdot 2H_2O$ in THF at room temperature, the PPh_3-monosubstituted complex [(μ-$SeCH_2)_2NC_6H_4OMe$-*p*]$Fe_2(CO)_5(PPh_3)$ (**6**) was produced (Scheme 3).

Scheme 3. Synthesis of Butterfly [2Fe2Se] Complexes 5 and 6

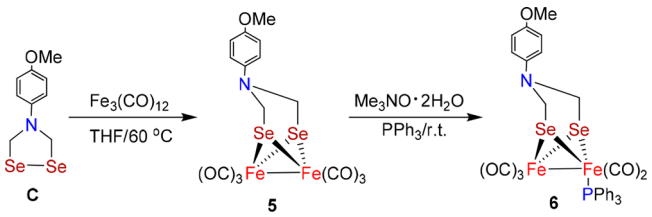

Table 1. Selected Bond Lengths (angstroms) and Angles (degrees) for 2 and 4

2			
S(1)−C(6)	1.8261(18)	Fe(2)−S(2)	2.2777(8)
S(1)−Fe(1)	2.2596(6)	Fe(2)−C(9)	1.9858(18)
S(1)−Fe(2)	2.2687(8)	Fe(1)−Fe(2)	2.5236(5)
S(2)−Fe(1)	2.2597(6)	C(9)−N(1)	1.377(2)
Fe(2)−S(1)−Fe(1)	67.737(16)	S(1)−Fe(1)−Fe(2)	56.30(2)
Fe(1)−S(2)−Fe(2)	67.581(15)	S(1)−Fe(2)−S(2)	84.641(18)
S(2)−Fe(1)−S(1)	85.27(2)	S(1)−Fe(2)−Fe(1)	55.959(17)
S(2)−Fe(1)−Fe(2)	56.55(2)	S(2)−Fe(2)−Fe(1)	55.868(17)
4			
Fe(1)−C(5)	2.099(6)	S(1)−Fe(1)	2.4508(16)
S(1)−Fe(2)	2.1392(16)	Fe(1)−Fe(2)	2.5245(11)
S(2)−Fe(1)	2.2256(16)	C(5)−N(1)	1.430(8)
S(2)−Fe(2)	2.3120(16)	Fe(2)−C(10)	2.066(6)
S(2)−Fe(1)−S(1)	84.01(5)	S(1)−Fe(2)−Fe(1)	62.77(5)
S(2)−Fe(1)−Fe(2)	57.84(4)	S(2)−Fe(2)−Fe(1)	54.58(4)
S(1)−Fe(1)−Fe(2)	50.90(4)	Fe(2)−S(1)−Fe(1)	66.33(5)
S(1)−Fe(2)−S(2)	89.42(6)	Fe(2)−S(2)−Fe(1)	67.58(5)

DOI: 10.1021/acs.organomet.9b00022
Organometallics XXXX, XXX, XXX−XXX

Interestingly, although the *N*-methoxyphenyl-substituted 1,2,4-diselenazolidine **C** reacted with $Fe_3(CO)_{12}$ to give the expected butterfly [2Fe2Se] complex **5**, the *N*-benzyl-, *N*-pyridylmethyl-, and *N*-ferrocenylmethyl-substituted 1,2,4-diselenazolidines **D**−**F**, respectively [note that the three diselenazolidines **D**−**F** and their precursors, 3,7-disubstituted 1,5,3,7-diselenadiazocanes **X**−**Z**, respectively, are new (see the Supporting Information for their synthesis and characterization)], were found to react with $Fe_3(CO)_{12}$ under similar conditions to give the first butterfly [2Fe1Se1N1C] core-containing complexes $[(\mu\text{-SeCH}_2)(\mu\text{-CH}_2\text{NR})]Fe_2(CO)_6$ (**7**, R = $PhCH_2$; **8**, R = $NC_5H_4CH_2$-*p*; **9**, R = $CpFeC_5H_4CH_2$), unexpectedly (Scheme 4).

Scheme 4. Synthesis of Butterfly [2Fe1Se1N1C] Complexes 7−9

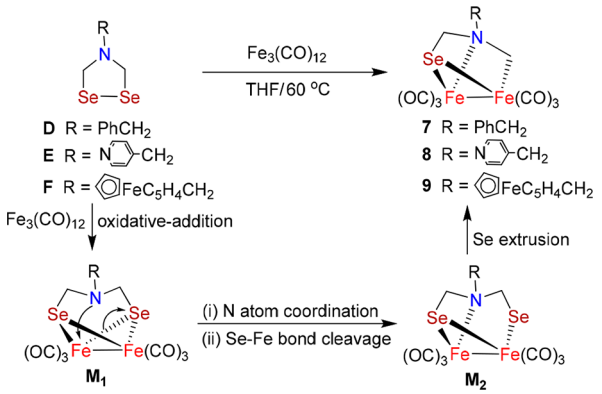

A possible pathway for the unexpected formation of complexes **7**−**9** is proposed in Scheme 4, which includes the following three major reaction steps. The first step, like the formation of complex **5**, involves oxidative addition of N-substituted 1,2,4-diselenazolidines **D**−**F** with $Fe_3(CO)_{12}$ to give butterfly [2Fe2Se] intermediates $\mathbf{M_1}$. The second step involves the intramolecular nucleophilic attack of N atoms in $\mathbf{M_1}$ (due to the fact that *N*-arylmethyl substituents in **D**−**F** are stronger electron-donating groups than the *N*-*p*-methoxyphenyl substituent in **C**) at one of their two Fe atoms with cleavage of one Se−Fe bond to give the seven-membered metallacycle (2Fe2Se1N2C)-containing intermediates $\mathbf{M_2}$. Actually, this step is very similar to the previously reported intramolecular nucleophilic attack at iron followed by loss of the Fe-bound ligand that occurred in some butterfly Fe/S cluster complexes.[44,45] The third step involves extrusion of one Se atom from the seven-membered metallacycle in $\mathbf{M_2}$ to give the more stable six-membered metallacycle (2Fe1Se1N2C)-containing butterfly [2Fe1Se1N1C] complexes **7**−**9**. The third step is actually similar to the previously reported extrusion of Se from the $p\text{-MeC}_6H_4SO_2Se$-bridged butterfly Fe/E complexes $(\mu\text{-RE})(\mu\text{-}p\text{-MeC}_6H_4SO_2Se)Fe_2(CO)_6$ (E = S or Se).[46] It should be noted that although this proposed pathway appears to be reasonable, some details for this pathway need to be further studied.

While complex **9** is an air-stable red oil, complexes **5**−**8** are air-stable red solids. The IR spectra of all-carbonyl complexes **5** and **7**−**9** showed three strong absorption bands in the range of 2060−1970 cm^{-1} for their terminal carbonyls; PPh_3-monosubstituted complex **6** displayed three bands in a much lower region of 2036−1921 cm^{-1}, obviously due to the increased intensity of π-back bonding between iron atoms and the attached carbonyls by CO substitution with the stronger σ-donor PPh_3.[47] The ^1H NMR spectra of **5** and **6** displayed one singlet at 3.80 and 3.72 ppm for their CH_3O groups, respectively, whereas those of **7**−**9** showed the corresponding multiplets for the H atoms in their benzene, pyridine, and cyclopentadienyl rings. The $^{77}Se\{^1H\}$ NMR spectra of complexes **5** and **6** exhibited one singlet at −103.6 ppm and two singlets at −276.6 and −263.9 ppm for their two Se atoms, respectively. The $^{77}Se\{^1H\}$ NMR spectra of complexes **7**−**9** displayed one singlet at 77.3, 71.4, and 84.6 ppm for their one Se atom, respectively.

The molecular structures of complexes **6** and **7** were unequivocally confirmed by X-ray crystallographic study. Figures 4 and 5 display their ORTEP views, whereas Table 2 lists their selected bond lengths and angles. As one can see in Figure 4, complex **6** contains an *N*-*p*-methoxyphenyl group-substituted ADSe ligand that is bridged between two iron atoms to form the two fused six-membered rings Fe(1)Se(1)-C(6)N(1)C(7)Se(2) and Fe(2)Se(2)C(7)N(1)C(6)Se(1) with a chair conformation and a boat conformation, respectively. The *p*-methoxyphenyl group in this butterfly [2Fe2Se] complex **6** is attached to the bridgehead N(1) atom via the common axial N(1)−C(8) bond of the two fused six-

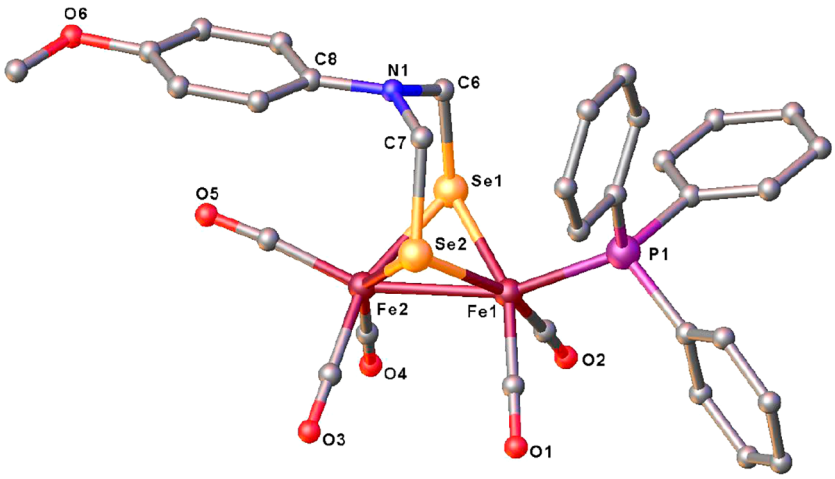

Figure 4. ORTEP view of **6** with 50% probability level ellipsoids. All hydrogen atoms have been omitted for the sake of clarity.

DOI: 10.1021/acs.organomet.9b00022
Organometallics XXXX, XXX, XXX−XXX

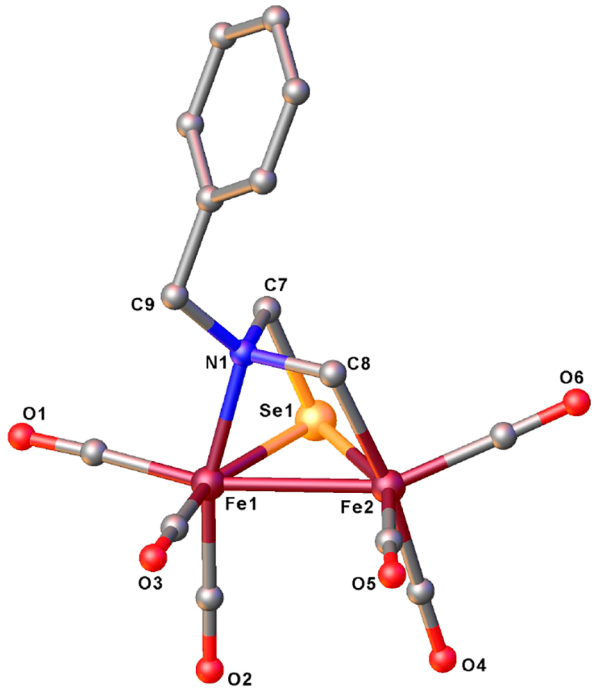

Figure 5. ORTEP view of **7** with 50% probability level ellipsoids. All hydrogen atoms have been omitted for the sake of clarity.

membered rings, to avoid the strong steric repulsions between the axially attached *p*-methoxyphenyl group and the bulky PPh_3 located in the apical position of the square-pyramidal Fe(1) atom. The Fe(1)−Fe(2) bond length (2.5497 Å) is very close to those of the previously reported ADSe-bridged diiron complexes.[33] As shown clearly in Figure 5, complex **7** indeed includes a butterfly [2Fe1Se1N1C] cluster core with a triangular Fe(1)Fe(2)Se(1) wing and a square-planar Fe(1)-Fe(2)C(8)N(1) wing. In addition, the methylene C(7) atom is bridged between N(1) and Se(1) atoms and the benzyl group is bound to the N(1) atom via the C(9)−N(1) bond. The Fe(1)−Fe(2) bond length is 2.5807 Å, which is longer than those of the butterfly [2Fe2Se] complex **6** and the previously reported ADSe-bridged diiron complexes.[33]

Synthesis and Characterization of the Parent ODTe-Bridged Butterfly [2Fe2Te] Complex and Its NHC-Substituted Derivatives. Although numerous butterfly [2Fe2S] and [2Fe2Se] core-containing [FeFe]-H_2 ase models have been reported previously,[20−35] only a few of the butterfly [2Fe2Te] core-containing [FeFe]-H_2 ase models have been prepared so far,[36,37] because they are less stable and more difficult to prepare in comparison to the corresponding butterfly Fe/S and Fe/Se complexes. We found that the first oxapropaneditellurolate (ODTe)-bridged type of butterfly [2Fe2Te] complex (μ-ODTe)$Fe_2(CO)_6$ (**10**) could be prepared by reductive cleavage of the Te−Te bond in ditellurium complex (μ-Te_2)$Fe_2(CO)_6$ with 2 equiv of Et_3BHLi in THF at −78 °C, followed by treatment of the resulting intermediate (μ-TeLi)$_2Fe_2(CO)_6$[7] from −78 to 60 °C with excess bis(chloromethyl) ether (Scheme 5).

Scheme 5. Synthesis of Parent Butterfly [2Fe2Te] Complex 10

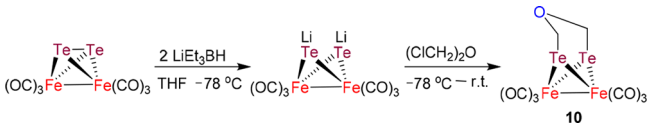

Having prepared the first ODTe-type model complex **10**, we found that the NHC-substituted and ODTe-bridged butterfly [2Fe2Te] complexes (μ-ODTe)$Fe_2(CO)_5(I_{Me/Mes})$ (**11**), (μ-ODTe)$Fe_2(CO)_5(I_{Mes})$ (**12**), and (μ-ODTe)$Fe_2(CO)_5(I_{Me})$ (**13**) were prepared (under conditions similar to those for preparation of the NHC-substituted and PDT-bridged butterfly [2Fe2S] complexes **1**−**4**) by CO substitution reactions of parent complex **10** with the NHC ligands $I_{Me/Mes}$, I_{Mes}, and I_{Me} generated in situ from the corresponding imidazolium salts under the action of *n*-BuLi or *t*-BuOK (Scheme 6).

While parent complex **10** is an air-stable red solid, its NHC-monosubstituted derivatives **11**−**13** are air-stable black solids. All of these new butterfly [2Fe2Te] complexes have been characterized by elemental analysis and various spectroscopies. For instance, the IR spectrum of parent complex **10** showed

Table 2. Selected Bond Lengths (angstroms) and Angles (degrees) for 6 and 7

6			
Se(1)−C(6)	2.027(4)	Fe(2)−Se(2)	2.3880(6)
Se(1)−Fe(1)	2.4046(7)	Fe(1)−P(1)	2.2469(10)
Se(1)−Fe(2)	2.3852(7)	Fe(1)−Fe(2)	2.5497(7)
Se(2)−Fe(1)	2.4045(7)	P(1)−C(15)	1.829(3)
Fe(2)−Se(1)−Fe(1)	64.322(19)	Se(2)−Fe(1)−Fe(2)	57.545(17)
Fe(1)−Se(2)−Fe(2)	64.28(2)	Se(1)−Fe(1)−Fe(2)	57.47(2)
P(1)−Fe(1)−Se(1)	109.69(3)	Se(1)−Fe(2)−Se(2)	85.60(2)
Se(2)−Fe(1)−Se(1)	84.81(2)	Se(1)−Fe(2)−Fe(1)	58.208(19)
7			
Se(1)−C(7)	1.963(2)	Se(1)−Fe(1)	2.3748(9)
Se(1)−Fe(2)	2.3656(6)	Fe(1)−Fe(2)	2.5807(7)
N(1)−Fe(1)	2.0451(19)	C(7)−N(1)	1.470(3)
C(8)−Fe(2)	2.069(2)	C(8)−N(1)	1.479(3)
C(7)−Se(1)−Fe(2)	95.45(8)	Se(1)−Fe(2)−Fe(1)	57.19(3)
C(7)−Se(1)−Fe(1)	76.37(7)	C(8)−Fe(2)−Se(1)	85.38(7)
Se(1)−Fe(1)−Fe(2)	56.845(19)	Fe(2)−Se(1)−Fe(1)	65.97(2)
N(1)−Fe(1)−Se(1)	72.76(6)	N(1)−Fe(1)−Fe(2)	74.39(6)

DOI: 10.1021/acs.organomet.9b00022
Organometallics XXXX, XXX, XXX−XXX

Scheme 6. Synthesis of NHC-Substituted Butterfly [2Fe2Te] Complexes 11−13

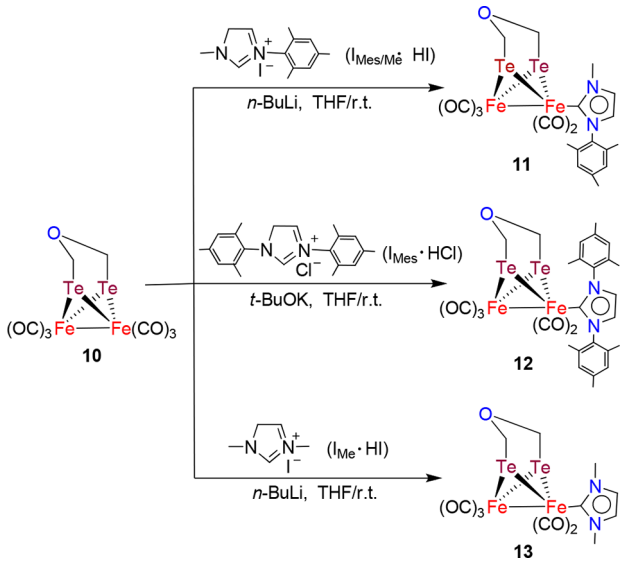

one medium and four strong absorption bands in the range of 2054−1949 cm^{-1} for its terminal carbonyls, whereas those of the NHC-monosubstituted derivatives **11**−**13** displayed three strong absorption bands in the region of 2016−1897 cm^{-1}. The three absorption bands displayed by **11**−**13** lie at a frequency range much lower than that displayed by their parent complex **10**, obviously due to the increased strength of the π-back bonding between the Fe atoms and the attached carbonyls by CO substitution with the stronger electron-donating NHC ligands.[38−40] The ^{1}H NMR spectra of complexes **10** and **11** displayed one singlet at 4.59 and 3.35 ppm for the two methylene groups in their ODTe ligands, whereas **12** and **13** exhibited one multiplet in the range of 4.05−4.58 ppm for their methylene groups in their ODTe ligands. The ^{13}C{^{1}H} NMR spectra of **11**−**13** showed one signal in the range of 182−199 ppm for their carbene C atoms.[31b,42] In addition, the ^{125}Te{^{1}H} NMR spectrum of **10** and its substituted derivative **12** showed one signal at −376.5 and −85.0 ppm for their two Te atoms, respectively.

To confirm the molecular structures of the ODTe-bridged butterfly [2Fe2Te] complexes **10**−**12** and to obtain the corresponding structural data, X-ray crystallographic studies of **10**−**12** were undertaken. The ORTEP views of **10**−**12** are depicted in Figures 6−8, respectively, while Table 3 presents their selected bond lengths and angles. Figures 6−8 demonstrate that the three complexes indeed have an ODTe ligand that is bridged between their two iron atoms. While the two iron atoms in parent complex **10** are all coordinated by three terminal CO ligands, one of the two iron atoms in the substituted complexes **11** and **12** is coordinated by three terminal CO ligands but another iron atom is by two terminal CO ligands and one NHC I$_{Me/Mes}$ or I$_{Mes}$ ligand. In addition, the NHC I$_{Me/Mes}$ ligand in **11** is located in a basal position of the square-pyramidal Fe(2) atom, whereas the NHC I$_{Mes}$ ligand in **12** is located in the apical position of the square-pyramidal Fe(2) atom. The Fe(1)−Fe(2) bond length of parent complex **10** (2.6324 Å) is slightly shorter than those of its substituted derivatives **11** (2.7084 Å) and **12** (2.6547 Å). In addition, the Fe(1)−Fe(2) bond length of the parent ODTe-type complex **10** (2.6324 Å) is longer than that of the parent

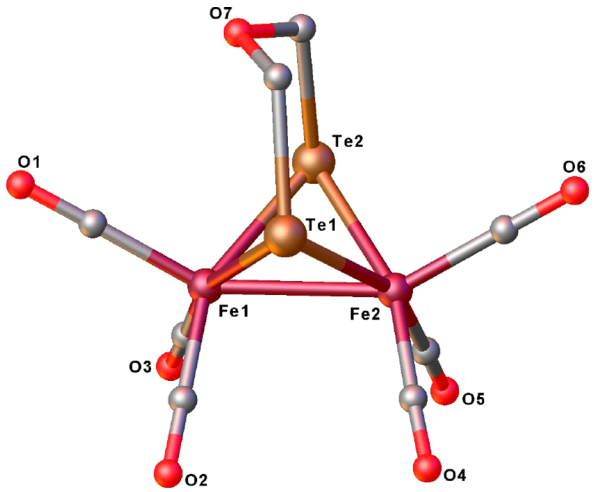

Figure 6. ORTEP view of **10** with 50% probability level ellipsoids. All hydrogen atoms have been omitted for the sake of clarity.

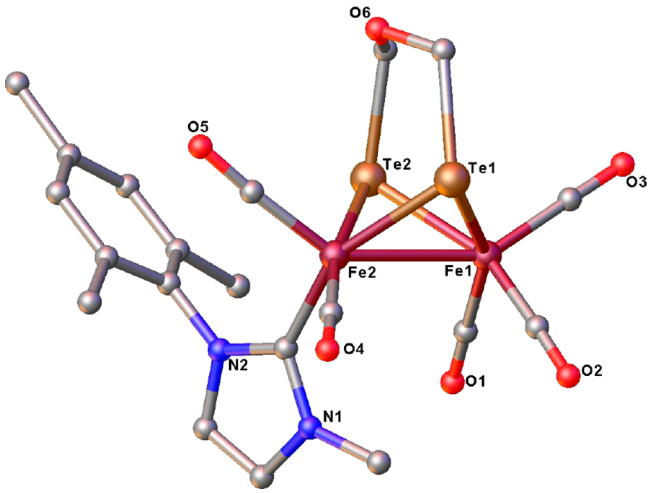

Figure 7. ORTEP view of **11** with 50% probability level ellipsoids. All hydrogen atoms have been omitted for the sake of clarity.

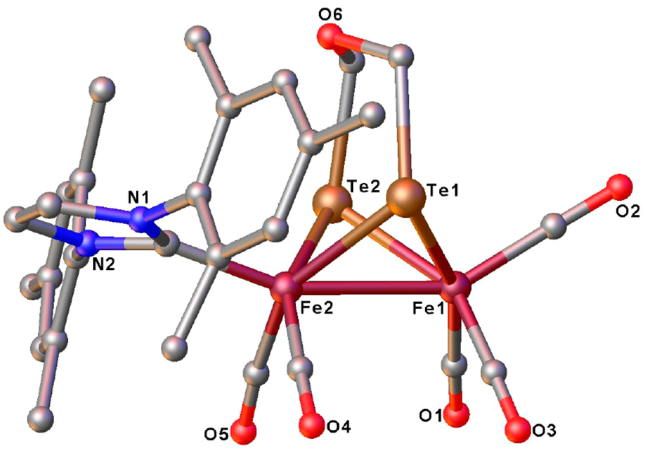

Figure 8. ORTEP view of **12** with 50% probability level ellipsoids. All hydrogen atoms have been omitted for the sake of clarity.

ODSe-type complex (2.5599 Å),[31b] and in turn, the Fe(1)−Fe(2) bond length of the parent ODSe-type complex is longer than that of the parent ODT (ODT = oxapropanedithiolate)-type complex (2.5113 Å),[28] because the atomic radii of the

DOI: 10.1021/acs.organomet.9b00022
Organometallics XXXX, XXX, XXX−XXX

Table 3. Selected Bond Lengths (angstroms) and Angles (degrees) for 10−12

10			
Te(1)−C(7)	2.190(5)	Fe(2)−Te(2)	2.5379(8)
Te(1)−Fe(1)	2.5428(8)	Te(2)−Fe(1)	2.5386(9)
Te(1)−Fe(2)	2.5343(9)	Fe(1)−Fe(2)	2.6324(10)
Te(2)−C(8)	2.185(5)	O(7)−C(7)	1.392(6)
C(7)−Te(1)−Fe(2)	110.20(14)	C(8)−Te(2)−Fe(1)	106.81(13)
C(7)−Te(1)−Fe(1)	105.86(13)	Fe(2)−Te(2)−Fe(1)	62.47(3)
Fe(2)−Te(1)−Fe(1)	62.46 (3)	Te(1)−Fe(1)−Fe(2)	58.61(3)
C(8)−Te(2)−Fe(2)	109.09(14)	Te(2)−Fe(2)−Te(1)	86.93(3)
11			
Te(1)−C(6)	2.186(3)	Fe(2)−Te(2)	2.5250(8)
Te(1)−Fe(1)	2.5319(7)	Te(2)−Fe(1)	2.5408(7)
Te(1)−Fe(2)	2.5252(8)	Fe(1)−Fe(2)	2.7084(8)
Fe(2)−C(11)	2.005(3)	C(11)−N(1)	1.361(4)
Fe(1)−Te(1)−Fe(2)	64.762(16)	Te(2)−Fe(1)−Fe(2)	57.40(2)
Fe(1)−Te(2)−Fe(2)	64.637(17)	Te(1)−Fe(2)−Te(2)	86.796(16)
Te(1)−Fe(1)−Te(2)	86.32(2)	Te(2)−Fe(2)−Fe(1)	57.963(18)
Te(1)−Fe(1)−Fe(2)	57.50(2)	Te(1)−Fe(2)−Fe(1)	57.74(2)
12			
Te(1)−C(6)	2.200(7)	Fe(2)−Te(2)	2.5627(16)
Te(1)−Fe(1)	2.5479(14)	Te(2)−Fe(1)	2.5606(15)
Te(1)−Fe(2)	2.5500(14)	Fe(1)−Fe(2)	2.6547(18)
Fe(2)−C(8)	1.997(6)	C(8)−N(1)	1.380(8)
Fe(1)−Te(1)−Fe(2)	62.77(4)	Te(2)−Fe(1)−Fe(2)	58.83(5)
Fe(1)−Te(2)−Fe(2)	62.42(4)	Te(1)−Fe(2)−Te(2)	86.55(4)
Te(1)−Fe(1)−Te(2)	86.64(4)	Te(1)−Fe(2)−Fe(1)	58.58(4)
Te(1)−Fe(1)−Fe(2)	58.66(3)	Te(2)−Fe(2)−Fe(1)	58.75(3)

three chalcogen atoms decrease in the following order: Te > Se > S.

Electrochemical and Electrocatalytic Studies of Model Complex 7. Although the electrochemical and electrocatalytic properties of some butterfly [2Fe2S],[23,25,30] [2Fe2Se],[33,34] and [2Fe2Te][36,37] models for [FeFe]-H_2 ases were previously studied by us and other groups, no electrochemical or electrocatalytic study of the butterfly [2Fe1Se1N1C] core-containing model complex has been reported until now. To determine the electrochemical and electrocatalytic properties of this type of model complex, we chose complex **7** as a representative to determine its electrochemical property and electrocatalytic ability. First, the electrochemical property of complex **7** was determined in MeCN with n-Bu_4NPF_6 as the electrolyte by cyclic voltammetry. As shown in Figure 9, the cyclic voltammogram of **7** consists of an irreversible reduction wave at −1.56 V, a reversible reduction wave at −1.70 V (ΔE_p = 80 mV; $i_{pa}/i_{pc} \approx 1$), and an irreversible oxidation wave at 0.40 V. Because the current function ($i_p/v^{1/2}$) values for the two reduction events of **7** remain constant at all scan rates (see Figures S9 and S10), each of the two reductions could be assigned to a one-electron reduction process from Fe^IFe^I to Fe^IFe^0 and from Fe^IFe^0 to Fe^0Fe^0 species.[48,49] However, because the current height of the oxidation peak of **7** is approximately twice that for each of its two reduction peaks, the oxidation event of **7** could be assigned to a two-electron oxidation process from Fe^IFe^I to $Fe^{II}Fe^{II}$ species.[28] It follows that such cyclic voltammetric behavior for **7** is very similar to that displayed by the previously reported butterfly [2Fe2Se] complexes [(μ-$SeCH_2)_2NC(O)$-R]$Fe_2(CO)_6$ (R = Me and Ph).[33] In addition, it is worth noting that the two reduction processes of **7** are diffusion-controlled because its two reduction peak currents versus the square root of the scan rates (25−1250 mV s^{-1}) are all linearly correlated (see Figure S11).[48]

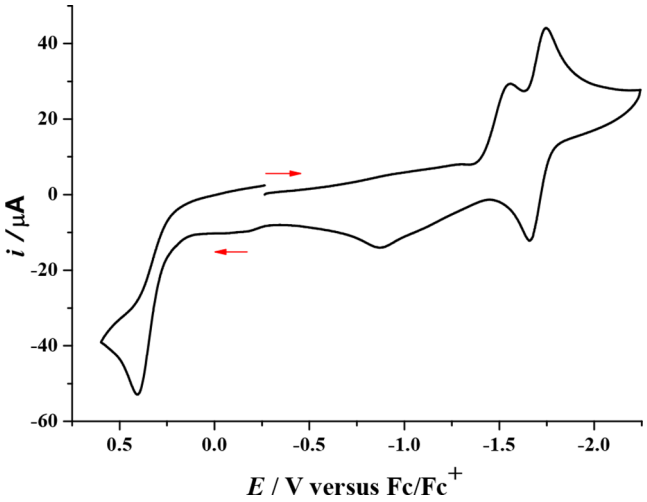

Figure 9. Cyclic voltammograms of **7** (1.0 mM) in 0.1 M n-Bu_4NPF_6/MeCN at a scan rate of 0.1 V s^{-1}. Arrows indicate the starting potential and scan direction.

To assess the electrocatalytic H_2-producing ability catalyzed by complex **7**, we recorded its cyclic voltammograms in the presence of benzoic acid $PhCO_2H$ (pK_a^{MeCN} = 20.7)[50] or p-toluenesulfonic acid TsOH (pK_a^{MeCN} = 8.7).[50] As shown in Figure 10, during addition of the weak acid $PhCO_2H$, the intensity of the original first reduction peak of **7** increased slightly, but the intensity of its original second reduction peak increased remarkably with continuous addition of the acid. However, in contrast to this, Figure 11 shows that during

DOI: 10.1021/acs.organomet.9b00022
Organometallics XXXX, XXX, XXX−XXX

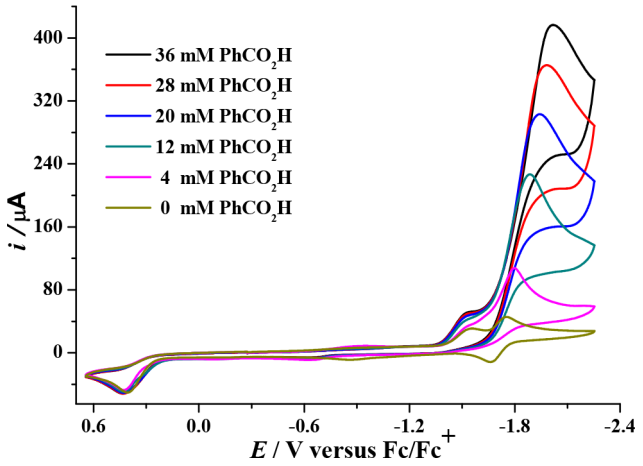

Figure 10. Cyclic voltammograms of **7** (1.0 mM) with varying amounts of $PhCO_2H$ in 0.1 M n-Bu_4NPF_6/MeCN at a scan rate of 0.1 V s^{-1}.

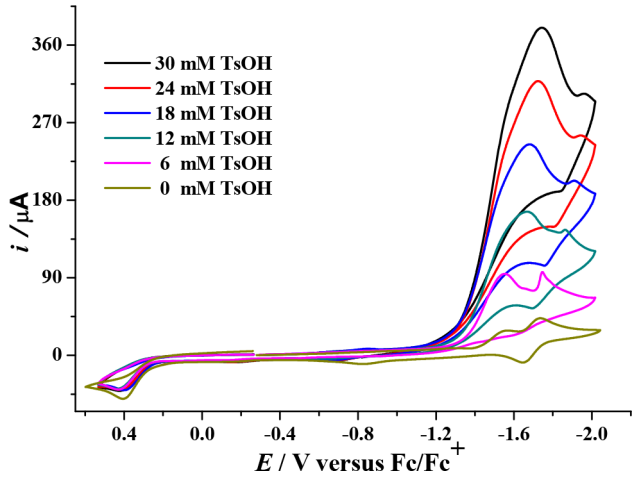

Figure 11. Cyclic voltammograms of **7** (1.0 mM) with varying amounts of TsOH in 0.1 M n-Bu_4NPF_6/MeCN at a scan rate of 0.1 V s^{-1}.

addition of the strong acid TsOH, the intensity of the original first reduction peak of **7** increased considerably with continuous addition of the acid, while that of its original second reduction peak was slightly increased. It is apparent that such observations demonstrated that complex **7** can act as the electrocatalyst for proton reduction to H_2 from $PhCO_2H$ and TsOH at its second and first reduction potentials, respectively.[28,30,35]

The electrocatalytic H_2-producing ability catalyzed by complex **7** was further confirmed by controlled-potential electrolysis (CPE) experiments of the MeCN solutions of **7** (0.5 mM) with excess $PhCO_2H$ (20 mM) at −2.15 V and TsOH (20 mM) at −1.88 V. During a 1 h CPE of **7** with $PhCO_2H$, a total of 32.6 F/mol of **7** passed, which corresponds to 16.3 turnovers (TONs); during a 1 h CPE of **7** with TsOH, a total of 35.4 F/mol of **7** passed, which corresponds to 17.7 TONs. It follows that the H_2-producing efficiencies catalyzed by **7** from $PhCO_2H$ and TsOH are much higher than those previously reported for the production of H_2 from HOAc catalyzed by the butterfly [2Fe2Se] model complexes $[(\mu\text{-}SeCH_2)_2X]Fe_2(CO)_6$ (X = O or S; TONs = 7.5 and 6.4, respectively).[31b]

SUMMARY AND CONCLUSIONS

Interestingly, four types of new model complexes (**1**−**13**) for [FeFe]-H_2 ases have been prepared by various synthetic methods. The first type of model complex (**1**−**4**) contains a PDT-bridged butterfly [2Fe2S] cluster core bearing five carbonyls and one NHC ligand or four carbonyls and two NHC ligands. While complexes **1**, **3**, and **4** are prepared by CO substitution reactions of **A** and **B** with the in situ-generated NHC ligands $I_{Me/Mes}$, I_{Mes}, and I_{Me} by loss of HX (X = Cl or I) from the corresponding imidazolium salts under the action of n-BuLi or t-BuOK, complex **2** is prepared by the CO substitution reaction of **A** with the NHC ligand $I_{Vinyl/Mes}$ generated unexpectedly by in situ thermal decomposition of the initially formed unstable dicarbene $I^*_{Mes}(CH_2)_2I^*_{Mes}$ from its HBr salt under the action of n-BuLi. The second type of model complex (**5** and **6**) has an ADSe-bridged butterfly [2Fe2Se] core bearing six carbonyls or five carbonyls and one PPh_3 ligand. While **5** is prepared by oxidative addition of N-methoxyphenyl-substituted diselenazolidine **C** with $Fe_3(CO)_{12}$, complex **6** is prepared by CO substitution of **5** with PPh_3. The third type of model complex (**7**−**9**) includes an azapropylselenolate ligand-bridged butterfly [2Fe1Se1N1C] cluster core bearing six carbonyl ligands. To our surprise, complexes **7**−**9** are obtained unexpectedly by reactions of the N-arylmethyl-substituted 1,2,4-diselenazolidines **D**−**F**, respectively, with $Fe_3(CO)_{12}$. Finally, the fourth type of model complex (**10**−**13**) contains an ODTe-bridged butterfly [2Fe2Te] cluster core carrying six carbonyls or five carbonyls and one NHC ligand. While complex **10** is prepared by condensation of intermediate $(\mu\text{-TeLi})_2Fe_2(CO)_6$ with bis(chloromethyl) ether, complexes **11**−**13** are prepared by CO substitution of complex **10** with the NHC ligands generated in situ from the corresponding imidazolium salts. All of the new model complexes **1**−**13** and the six new starting materials **D**−**F** and **X**−**Z** used for preparation of complexes **7**−**9** are characterized by elemental analysis and spectroscopy, and in particular, the molecular structures of some of their representatives are confirmed by X-ray crystal diffraction analysis. Finally, it should be indicated that complex **7** as one representative of the first butterfly [2Fe1Se1N1C] cluster core-containing complexes **7**−**9** has been found to be an electrocatalyst for the production of H_2 from $PhCO_2H$ and p-$MeC_6H_4SO_3H$ under cyclic voltammetry conditions.

EXPERIMENTAL SECTION

General Comments. All reactions were carried out using standard Schlenk and vacuum-line techniques under an atmosphere of highly purified nitrogen. THF was purified by distillation under N_2 from sodium/benzophenone ketyl. Et_3BHLi (1 M in THF), n-BuLi (2.5 M in hexane), t-BuOK, $Me_3NO{\cdot}2H_2O$, Ph_3P, and $(ClCH_2)_2O$ were available commercially and used as received. $Fe_3(CO)_{12}$,[51] 1,3-bis(mesityl)imidazolium chloride ($I_{Mes}{\cdot}HCl$),[52] 1,3-dimethylimidazolium iodide ($I_{Me}{\cdot}HI$),[53] 1-mesityl-3-methylimidazolium iodide ($I_{Me/Mes}{\cdot}HI$),[41] 1,2-bis(mesitylimidazolium)ethane dibromide $[I^*_{Mes}(CH_2)_2I^*_{Mes}{\cdot}2HBr]$,[54] $[(\mu\text{-}SCH_2)_2CH_2]Fe_2(CO)_6$ (**A**),[2] $[(\mu\text{-}SCH_2)_2CHO_2CPh]Fe_2(CO)_6$ (**B**),[55] $(\mu\text{-}Te_2)Fe_2(CO)_6$,[56] and N-p-$MeOC_6H_4$-substituted 1,2,4-diselenazolidine (**C**)[43] were prepared according to the published procedures. The three new starting materials N-benzyl-1,2,4-diselenazolidine (**D**), N-pyridylmethyl-1,2,4-diselenazolidine (**E**), and N-ferrocenylmethyl-1,2,4-diselenazolidine (**F**) for preparation of complexes $[(\mu\text{-}SeCH_2)(\mu\text{-}CH_2NR)]Fe_2(CO)_6$ (**7**, R = $PhCH_2$; **8**, R = $NC_5H_4CH_2$-p; **9**, R = $CpFeC_5H_4CH_2$) as well as three new starting materials 3,7-dibenzyl-1,5,3,7-diselenadiazocane (**X**), 3,7-dipyridylmethyl-1,5,3,7-diselenadiazocane (**Y**), and 3,7-

DOI: 10.1021/acs.organomet.9b00022
Organometallics XXXX, XXX, XXX−XXX

Table 4. Crystal Data and Structural Refinement Details for 2 and 4

	2	4
molecular formula	$C_{22}H_{22}Fe_2N_2O_5S_2$	$C_{24}H_{26}Fe_2N_4O_6S_2 \cdot CH_2Cl_2$
molecular weightt	570.24	727.23
crystal system	triclinic	monoclinic
space group	$P\bar{1}$	$P121/n1$
a (Å)	8.086(2)	8.4738(7)
b (Å)	8.454(2)	12.0771(8)
c (Å)	17.831(5)	29.2415(19)
α (deg)	101.749(4)	90
β (deg)	90.301(4)	94.698(4)
γ (deg)	97.898(5)	90
V (Å^3)	1181.5(6)	2982.5(4)
Z	2	4
D_c (g cm^{-3})	1.603	1.620
absorption coefficient (mm^{-1})	1.441	1.338
$F(000)$	584	1488
index ranges	$-10 \le h \le 10$, $-11 \le k \le 10$, $-23 \le l \le 23$	$-10 \le h \le 10$, $-14 \le k \le 14$, $-34 \le l \le 34$
no. of reflections	14972	20293
no. of independent reflections	5622	5234
$2\theta_{max}$ (deg)	2.33/27.91	1.83/25.00
R	0.0272	0.0688
R_w	0.0678	0.1767
goodness of fit	1.022	1.087
largest difference peak/hole (e Å^{-3})	0.350/−0.311	1.315/−1.125

Table 5. Crystal Data and Structural Refinement Details for 6 and 7

	6	7
molecular formula	$C_{32}H_{26}Fe_2NO_6PSe_2 \cdot CH_2Cl_2$	$C_{15}H_{11}Fe_2NO_6Se$
molecular weight	906.05	491.91
crystal system	monoclinic	monoclinic
space group	$P121/c1$	$P2(1)/c$
a (Å)	9.3144(15)	9.2923(19)
b (Å)	10.3083(16)	13.806(3)
c (Å)	36.214(6)	13.961(3)
α (deg)	90	90
β (deg)	93.833(3)	101.73(3)
γ (deg)	90	90
V (Å^3)	3469.3(10)	1753.7(6)
Z	4	4
D_c (g cm^{-3})	1.735	1.863
absorption coefficient (mm^{-1})	3.180	3.760
$F(000)$	1800	968
index ranges	$-11 \le h \le 11$, $-13 \le k \le 9$, $-46 \le l \le 46$	$-9 \le h \le 12$, $-18 \le k \le 17$, $-16 \le l \le 18$
no. of reflections	30551	15470
no. of independent reflections	7648	4171
$2\theta_{max}$ (deg)	2.05/27.20	2.10/27.88
R	0.0454	0.0362
R_w	0.0821	0.0708
goodness of fit	1.074	1.098
largest diff peak/hole (e Å^{-3})	0.712/−0.615	0.544/−0.621

diferrocenylmethyl-1,5,3,7-diselenadiazocane (**Z**) for preparation of diselenazolidines **D**−**F**, respectively, were prepared and characterized (see the Supporting Information). Preparative thin layer chromatography (TLC) was carried out on glass plates (26 cm × 20 cm × 0.25 cm) coated with silica gel H (10−40 μm). IR spectra were recorded on a Bio-Rad FTS 135 or Bruker Tensor 27 FTIR spectrophotometer. ^{1}H (^{13}C, ^{31}P, ^{77}Se, ^{125}Te) NMR spectra were obtained on a Bruker Avance 300 NMR or 400 NMR spectrometer. Analysis and assignments of the ^{1}H NMR spectral data of complexes **7**−**9** were supported by ^{13}C−^{1}H HMQC (heteronuclear multiple-quantum correlation) and ^{13}C−^{1}H HMBC (heteronuclear multiple-bond correlation) spectra (see the Supporting Information). Elemental analyses were performed on an Elementar Vario EL analyzer. Melting points were determined on a Yanaco Mp-500 or a SGW X-4 microscopic melting point apparatus and are uncorrected.

Preparation of [(μ-SCH$_2$)$_2$CH$_2$]Fe$_2$(CO)$_5$(I$_{Me/Mes}$) (1). *n*-BuLi (0.8 mL, 2.0 mmol) was added in a dropwise manner by a syringe to a stirred suspension of the imidazolium salt $I_{Me/Mes}$·HI (0.500 g, 1.52 mmol) in THF (10 mL) to give a yellowish solution. After the solution was stirred at room temperature for an additional 15 min, it was filtered under anaerobic conditions through a Celite-packed column and eluted with THF (15 mL) to give a filtrate containing the air-sensitive NHC ligand $I_{Me/Mes}$. To this filtrate was added [(μ-SCH$_2$)$_2$CH$_2$]Fe$_2$(CO)$_6$ (**A**) (0.386 g, 1.00 mmol), and the new mixture was stirred at room temperature for 4 h until **A** had been completely consumed as indicated by TLC. The solvent was removed at reduced pressure, and then the residue was subjected to TLC separation using CH$_2$Cl$_2$/petroleum ether [1:7 (v/v)] as the eluent. From the main red band, **1** (0.452 g, 81%) was obtained as a red solid: mp 171−173 °C; IR (KBr disk) $\nu_{C\equiv O}$ 2030 (vs), 1957 (vs), 1911 (s) cm^{-1}; ^{1}H NMR (300 MHz, CDCl$_3$) δ 1.64−1.89 (m, 6H, CH$_2$CH$_2$CH$_2$), 2.10 (s, 6H, 2-*o*-CH$_3$ of C$_6$H$_2$), 2.36 (s, 3H, *p*-CH$_3$ of C$_6$H$_2$), 4.04 (s, 3H, NCH$_3$), 6.87−7.12 (m, 4H, NCH═CHN, C$_6$H$_2$); ^{13}C{^{1}H} NMR (75 MHz, CDCl$_3$) δ 18.6 (s, *o*-CH$_3$ of C$_6$H$_2$), 21.2 (s, *p*-CH$_3$ of C$_6$H$_2$), 29.7, 39.6 (2s, CH$_2$CH$_2$CH$_2$), 123.7, 124.2 (2s, NCH═CHN), 129.2−139.0 (m, C$_6$H$_2$), 189.0 (s, NCN), 211.2, 215.6 (2s, C≡O). Anal. Calcd for $C_{21}H_{22}Fe_2N_2O_5S_2$: C, 45.18; H, 3.97; N, 5.02. Found: C, 45.38; H, 4.02; N, 4.95.

Preparation of [(μ-SCH$_2$)$_2$CH$_2$]Fe$_2$(CO)$_5$(I$_{Vinyl/Mes}$) (2). To a stirred suspension of the imidazolium salt I*$_{Mes}$(CH$_2$)$_2$I*$_{Mes}$·2HBr (0.756 g, 1.35 mmol) in THF (20 mL) was added *n*-BuLi (1.1 mL, 2.75 mmol) in a dropwise manner by a syringe to give an orange-red solution. After the solution was stirred at room temperature for an additional 45 min, it was filtered under anaerobic conditions through a Celite-packed column and eluted with THF (15 mL) to give a filtrate containing the air-sensitive NHC ligand $I_{Vi/Mes}$. To this filtrate was added complex **A** (0.259 g, 0.67 mmol), and the new mixture was stirred at room temperature for 6 h until **A** had been completely consumed. The solvent was removed at reduced pressure, and then the residue was subjected to TLC separation using CH$_2$Cl$_2$/petroleum ether [1:5 (v/v)] as the eluent. From the main red band, **2** (0.172 g, 45%) was obtained as a red solid: mp 197−199 °C; IR (KBr disk) $\nu_{C\equiv O}$ 2035 (vs), 1963 (vs), 1910 (s) cm^{-1}; ^{1}H NMR (300 MHz, CDCl$_3$) δ 1.68−2.04 (m, 6H, CH$_2$CH$_2$CH$_2$), 2.12 (s, 6H, 2-*o*-CH$_3$ of C$_6$H$_2$), 2.36 (s, 3H, *p*-CH$_3$ of C$_6$H$_2$), 5.07−5.30 (m, 3H, NCH═CH$_2$), 6.95−7.50 (m, 4H, NCH═CHN, C$_6$H$_2$); ^{13}C{^{1}H} NMR (75 MHz, CDCl$_3$) δ 18.4 (s, *o*-CH$_3$ of C$_6$H$_2$), 21.2 (s, *p*-CH$_3$ of C$_6$H$_2$), 23.8, 29.6 (2s, CH$_2$CH$_2$CH$_2$), 102.6, 119.2 (2s, NCH═CH$_2$), 124.8 (s, NCH═CHN), 129.3−139.3 (m, C$_6$H$_2$), 193.7 (s, NCN), 210.7, 214.8 (2s, C≡O). Anal. Calcd for $C_{22}H_{22}Fe_2N_2O_5S_2$: C, 46.34; H, 3.89; N, 4.91. Found: C, 46.39; H, 4.01; N, 4.71.

Preparation of [(μ-SCH$_2$)$_2$CHO$_2$CPh]Fe$_2$(CO)$_5$(I$_{Mes}$) (3). To a stirred suspension of the imidazolium salt I_{Mes}·HCl (0.300 g, 0.88 mmol) in THF (15 mL) was added *n*-BuLi (0.6 mL, 1.50 mmol) in a dropwise manner by a syringe to give a yellow solution. After the solution was stirred at room temperature for an additional 15 min, it

DOI: 10.1021/acs.organomet.9b00022
Organometallics XXXX, XXX, XXX−XXX

Table 6. Crystal Data and Structural Refinement Details for 10−12

	10	11	12
molecular formula	$C_8H_4Fe_2O_7Te_2$	$C_{20}H_{20}Fe_2N_2O_6Te_2$	$C_{28}H_{28}Fe_2N_2O_6Te_2$
molecular weight	579.01	751.28	855.42
crystal system	monoclinic	monoclinic	triclinic
space group	$P2(1)/c$	$P2(1)/n$	$P\bar{1}$
a (Å)	10.062(2)	8.990(3)	8.755(5)
b (Å)	8.2258(16)	20.439(6)	10.782(6)
c (Å)	17.237(3)	13.088(4)	17.784(10)
α (deg)	90	90	102.576(6)
β (deg)	95.18(3)	93.303(5)	93.072(3)
γ (deg)	90	90	111.666(10)
V (Å^3)	1420.9(5)	2400.8(12)	1506.2(14)
Z	4	4	2
D_c (g cm^{-3})	2.070	2.079	1.886
absorption coefficient (mm^{-1})	6.087	3.628	2.905
$F(000)$	1056	1432	828
index ranges	$-11 \le h \le 9, -9 \le k \le 9, -20 \le l \le 20$	$-11 \le h \le 11, -26 \le k \le 26, -17 \le l \le 15$	$-11 \le h \le 11, -14 \le k \le 9, -23 \le l \le 23$
no. of reflections	9783	24920	14631
no. of independent reflections	2487	5676	7091
$2\theta_{max}$ (deg)	2.37/25.01	1.85/27.84	2.10/27.87
R	0.0301	0.0260	0.0642
R_w	0.0712	0.0548	0.1360
goodness of fit	1.014	1.014	1.071
largest diff peak/hole (e Å^{-3})	0.763/−0.756	0.606/−1.118	1.108/−1.528

was filtered through an anaerobic Celite-packed column and then eluted with THF (15 mL) to give a filtrate containing the air-sensitive NHC ligand I_{Mes}. To this filtrate was added $[(\mu\text{-}SCH_2)_2CHO_2CPh]\text{-}Fe_2(CO)_6$ (**B**) (0.120 g, 0.25 mmol), and the new mixture was stirred at room temperature for 6 h until **B** had been completely consumed as indicated by TLC. The solvent was removed at reduced pressure, and then the residue was subjected to TLC separation using CH_2Cl_2/petroleum ether [1:4 (v/v)] as the eluent. From the main red band, complex **3** (0.086 g, 44%) was obtained as a red solid: mp 191−193 °C; IR (KBr disk) $\nu_{C\equiv O}$ 2037 (vs), 1972 (vs), 1948 (s), 1920 (s) cm^{-1}; IR (KBr disk) $\nu_{C=O}$ 1709 (s) cm^{-1}; ^{1}H NMR (300 MHz, $CDCl_3$) δ 1.53−2.50 (m, 22H, $2SCH_2$, $6CH_3$), 3.33−3.45 (m, 1H, CH), 6.95−8.03 (m, 11H, NCH═CHN, C_6H_5, $2C_6H_2$); $^{13}C\{^1H\}$ NMR (75 MHz, $CDCl_3$) δ 18.6 (s, o-CH_3 of C_6H_2), 21.2 (s, p-CH_3 of C_6H_2), 29.2 (s, SCH_2), 75.1 (s, OCH), 125.1 (s, NCH═CHN), 128.4−139.4 (m, C_6H_2), 164.5 (s, OC═O), 190.3 (s, NCN), 214.4 (s, C≡O). Anal. Calcd for $C_{36}H_{34}Fe_2N_2O_7S_2$: C, 55.26; H, 4.38; N, 3.58. Found: C, 55.24; H, 4.39; N, 3.32.

Preparation of $[(\mu\text{-}SCH_2)_2CHO_2CPh]Fe_2(CO)_4(I_{Me})_2$ (4). To a stirred suspension of the imidazolium salt $I_{Me}\cdot HI$ (1.120 g, 4.80 mmol) in THF (20 mL) was added t-BuOK (0.672 g, 6.00 mmol). After the mixture was stirred at room temperature for 2 h, it was filtered through an anaerobic Celite-packed column and then eluted with THF (20 mL) to give a filtrate containing the air-sensitive free carbene I_{Me}. To this filtrate was added complex **B** (0.400 g, 0.84 mmol), and the new mixture was stirred at room temperature for 2 h until **B** had been completely consumed. The solvent was removed at reduced pressure, and then the residue was subjected to TLC separation using CH_2Cl_2/petroleum ether [2:1 (v/v)] as the eluent. From the main red band, **4** (0.218 g, 42%) was obtained as a red solid: mp 256 °C dec; IR (KBr disk) $\nu_{C\equiv O}$ 1961 (s), 1924 (vs), 1901 (s), 1871 (s) cm^{-1}; IR (KBr disk) $\nu_{C=O}$ 1714 (s) cm^{-1}; ^{1}H NMR (300 MHz, $CDCl_3$) δ 1.54, 2.53 (2br s, 4H, $2SCH_2$), 4.08 (br s, 13H, CH, $4NCH_3$, OCH), 6.94−7.03 (m, 4H, 2NCH═CHN), 7.35−7.82 (m, 5H, C_6H_5). Anal. Calcd for $C_{24}H_{26}Fe_2N_4O_6S_2$: C, 44.88; H, 4.08; N, 8.72. Found: C, 44.99; H, 4.05; N, 8.73.

Preparation of $[(\mu\text{-}SeCH_2)_2NC_6H_4OMe\text{-}p]Fe_2(CO)_6$ (5). A mixture of the N-p-methoxymethyl-substituted 1,2,4-diselenazolidine (**C**, 0.62 g, 2.0 mmol) and $Fe_3(CO)_{12}$ (1.00 g, 2.0 mmol) in THF (30 mL) was heated to 60 °C and stirred at this temperature for 2.5 h. After removal of the solvent at reduced pressure, the residue was subjected to TLC separation using CH_2Cl_2/petroleum ether [1:5 (v/v)] as the eluent. From the orange-red band, **5** (0.230 g, 20%) was obtained as a red solid: mp 146 °C dec; IR (KBr disk) $\nu_{C\equiv O}$ 2060 (s), 2016 (vs), 1987 (vs), 1970 (vs) cm^{-1}; ^{1}H NMR (400 MHz, $CDCl_3$) δ 3.80 (s, 3H, OCH_3), 4.52 (br s, 4H, CH_2NCH_2), 6.78, 6.91 (dd, J = 10.0 Hz, 4H, C_6H_4); $^{77}Se\{^1H\}$ (76 MHz, $CDCl_3$, Me_2Se) δ −103.6 (s). Anal. Calcd for $C_{15}H_{11}Fe_2NO_7Se_2$: C, 30.70; H, 1.89; N, 2.39. Found: C, 30.94; H, 1.98; N, 2.26.

Preparation of $[(\mu\text{-}SeCH_2)_2NC_6H_4OMe\text{-}p]Fe_2(CO)_5(PPh_3)$ (6). A mixture of **5** (0.120 g, 0.20 mmol) and decarbonylating agent $Me_3NO\cdot 2H_2O$ (0.030 g, 0.27 mmol) in Me_3CN (20 mL) was stirred at room temperature for 10 min, and then PPh_3 (0.054 g, 0.20 mmol) was added. After the new mixture was stirred for an additional 2 h, the solvent was removed at reduced pressure and then the residue was subjected to TLC separation using CH_2Cl_2/petroleum ether [1:1 (v/v)] as the eluent. From the orange-red band, **6** (0.090 g, 55%) was obtained as a red solid: mp 155 °C dec; IR (KBr disk) $\nu_{C\equiv O}$ 2036 (vs), 1978 (vs), 1921 (s) cm^{-1}; ^{1}H NMR (400 MHz, acetone-d_6) δ 2.83, 4.40 (dd, J = 12.0 Hz, 4H, CH_2NCH_2), 3.72 (s, 3H, OCH_3), 6.86 (s, 4H, C_6H_4), 7.57−7.86 (m, 15H, $3C_6H_5$); $^{77}Se\{^1H\}$ (76 MHz, $CDCl_3$, Me_2Se) δ −263.9 (s), −276.6 (s); $^{31}P\{^1H\}$ NMR (162 MHz, acetone-d_6, H_3PO_4) δ 68.2 (s). Anal. Calcd for $C_{32}H_{26}Fe_2NO_6PSe_2$: C, 46.81; H, 3.19; N, 1.71. Found: C, 46.63; H, 3.17; N, 1.64.

Preparation of $[(\mu\text{-}SeCH_2)(\mu\text{-}CH_2NCH_2Ph)]Fe_2(CO)_6$ (7). A mixture of the N-benzyl-substituted 1,2,4-diselenazolidine (**D**, 0.59 g, 2.0 mmol) and $Fe_3(CO)_{12}$ (1.00 g, 2.0 mmol) in THF (30 mL) was heated to 60 °C and stirred at this temperature for 2 h. After removal of the solvent at reduced pressure, the residue was subjected to TLC separation using CH_2Cl_2/petroleum ether [1:6 (v/v)] as the eluent. From the major orange-red band, **7** (0.200 g, 20%) was obtained as a red solid: mp 107−108 °C; IR (KBr disk) $\nu_{C\equiv O}$ 2060 (s), 2012 (vs), 1971 (vs) cm^{-1}; ^{1}H NMR (400 MHz, acetone-d_6) δ 2.57, 3.35 (dd, J = 8.0 Hz, 2H, NCH_2Fe), 2.98, 5.20 (dd, J = 8.0 Hz, 2H, NCH_2Se), 3.54, 3.69 (dd, J = 14.0 Hz, 2H, $C_6H_5CH_2N$), 7.38−7.40 (m, 5H, C_6H_5); $^{77}Se\{^1H\}$ (76 MHz, $CDCl_3$, Me_2Se) δ 77.3 (s). Anal. Calcd for $C_{15}H_{11}Fe_2NO_6Se$: C, 36.63; H, 2.25; N, 2.85. Found: C, 36.67; H, 2.40; N, 2.61.

DOI: 10.1021/acs.organomet.9b00022
Organometallics XXXX, XXX, XXX−XXX

Preparation of [(μ-SeCH$_2$)(μ-CH$_2$N-*p*-CH$_2$C$_5$H$_4$N)]Fe$_2$(CO)$_6$ (8). A mixture of *N*-pyridylmethyl-substituted 1,2,4-diselenazolidine (**E**, 0.58 g, 2.0 mmol) and Fe$_3$(CO)$_{12}$ (1.00 g, 2.0 mmol) in THF (30 mL) was heated to 60 °C and then stirred at this temperature for 2.5 h. After removal of the solvent at reduced pressure, the residue was subjected to TLC separation using CH$_2$Cl$_2$/petroleum ether [1:6 (v/v)] as the eluent. From the major orange-red band, **8** (0.180 g, 18%) was obtained as a red solid: mp 120−121 °C; IR (KBr disk) $\nu_{C\equiv O}$ 2060 (s), 2013 (vs), 1973 (s) cm^{-1}; ^{1}H NMR (400 MHz, acetone-d_6) δ 2.61, 3.36 (2s, 2H, NCH$_2$Fe), 3.02, 5.26 (2s, 2H, NCH$_2$Se), 3.59, 3.77 (dd, J = 12.0 Hz, 2H, NC$_5$H$_4$C*H*$_2$N), 7.40, 8.58 (2s, 4H, NC$_5$H$_4$); ^{77}Se{^{1}H} (76 MHz, CDCl$_3$, Me$_2$Se) δ 71.4 (s). Anal. Calcd for C$_{14}$H$_{10}$Fe$_2$N$_2$O$_6$Se: C, 34.12; H, 2.04; N, 5.68. Found: C, 34.03; H, 2.30; N, 5.35.

Preparation of [(μ-SeCH$_2$)(μ-CH$_2$NCH$_2$C$_5$H$_4$FeCp)]Fe$_2$(CO)$_6$ (9). A mixture of *N*-ferrocenylmethyl-substituted 1,2,4-diselenazolidine (**F**, 0.63 g, 1.57 mmol) and Fe$_3$(CO)$_{12}$ (1.00 g, 2.0 mmol) in THF (30 mL) was heated to 60 °C and stirred at this temperature for 2 h. After removal of the solvent in vacuo, the residue was subjected to TLC separation using CH$_2$Cl$_2$/petroleum ether [1:4 (v/v)] as the eluent. From the major orange-red band, **9** was obtained as a red oil (0.200 g, 21%): IR (KBr disk) $\nu_{C\equiv O}$ 2058 (s), 2011 (vs), 1970 (vs) cm^{-1}; ^{1}H NMR (400 MHz, CDCl$_3$) δ 2.56, 3.02 (dd, J = 4.0 Hz, 2H, NCH$_2$Fe), 2.83, 4.53 (2s, 2H, NCH$_2$Se), 3.17, 3.26 (dd, J = 14.0 Hz, 2H, C$_5$H$_4$C*H*$_2$N), 4.10−4.22 (m, 9H, C$_5$H$_4$, C$_5$H$_5$); ^{77}Se{^{1}H} (76 MHz, CDCl$_3$, Me$_2$Se) δ 84.6 (s). Anal. Calcd for C$_{19}$H$_{15}$Fe$_3$NO$_6$Se: C, 38.05; H, 2.52; N, 2.34. Found: C, 38.15; H, 2.64; N, 2.10.

Preparation of [(μ-TeCH$_2$)$_2$O]Fe$_2$(CO)$_6$ (10). A petroleum ether solution (20 mL) containing (μ-Te$_2$)Fe$_2$(CO)$_6$ (0.290 g, 0.50 mmol) was mixed with THF (20 mL) and then cooled to −78 °C with a liquid N$_2$/acetone bath. LiEt$_3$BH (1.0 mL, 1.0 mmol) was added in a dropwise manner to this stirred solution by a syringe. At the midpoint of the addition, the reaction solution turned from orange-red to dark green, and for the rest of the addition, it gradually became brown-red. After the resulting solution was warmed to room temperature, (ClCH$_2$)$_2$O (90 μL) was added. The new mixture was heated to 60 °C and then stirred at this temperature for 12 h. The solvent was removed at reduced pressure, and the residue was subjected to TLC separation using CH$_2$Cl$_2$/petroleum ether [v/v (1:6)] as the eluent. From the second main red band, **10** (0.060 g, 21%) was obtained as a red solid: mp 135 °C dec; IR (KBr disk) $\nu_{C\equiv O}$ 2054 (m), 2010 (s), 1987 (vs), 1962 (s), 1949 (s) cm^{-1}; ^{1}H NMR (300 MHz, CDCl$_3$) δ 4.59 (s, 4H, CH$_2$OCH$_2$); ^{125}Te{^{1}H} NMR (126 MHz, CDCl$_3$, Me$_2$Te) δ −376.5. Anal. Calcd for C$_8$H$_4$Fe$_2$O$_7$Te$_2$: C, 16.60; H, 0.70. Found: C, 16.58; H, 0.67.

Preparation of [(μ-TeCH$_2$)$_2$O]Fe$_2$(CO)$_5$(I$_{Me/Mes}$) (11). *n*-BuLi (0.7 mL, 1.75 mmol) was slowly added at room temperature to a stirred suspension of the imidazolium salt I$_{Me/Mes}$·HI (0.262 g, 0.80 mmol) in THF (15 mL) to give a yellow solution. After the solution was stirred at this temperature for an additional 15 min, complex **10** (0.058 g, 0.10 mmol) was added. The new mixture was stirred at room temperature for 1.5 h until **10** had been completely consumed as indicated by TLC. The solvent was removed at reduced pressure, and then the residue was subjected to TLC separation using CH$_2$Cl$_2$/petroleum ether [1:3 (v/v)] as the eluent. From the main black band, **11** (0.029 g, 39%) was obtained as a black solid: mp 149−151 °C; IR (KBr disk) $\nu_{C\equiv O}$ 2014 (s), 1954 (vs), 1901 (s) cm^{-1}; ^{1}H NMR (400 MHz, CDCl$_3$) δ 2.17 (s, 6H, 2-*o*-CH$_3$ of C$_6$H$_2$), 2.39 (s, 3H, *p*-CH$_3$ of C$_6$H$_2$), 3.82 (br s, 3H, NCH$_3$), 4.35 (br s, 4H, CH$_2$OCH$_2$), 6.88−7.10 (m, 4H, NCH═CHN, C$_6$H$_2$); ^{13}C{^{1}H} NMR (100 MHz, CDCl$_3$) δ 19.3 (s, *o*-CH$_3$ of C$_6$H$_2$), 21.2 (s, *p*-CH$_3$ of C$_6$H$_2$), 40.7 (s, NCH$_3$), 44.5 (s, CH$_2$OCH$_2$), 124.2 (s, NCH═CHN), 129.6−139.2 (m, C$_6$H$_2$), 189.1 (s, NCN), 213.5, 217.2 (2s, C≡O). Anal. Calcd for C$_{20}$H$_{20}$Fe$_2$N$_2$O$_6$Te$_2$: C, 31.97; H, 2.68; N, 3.73. Found: C, 32.10; H, 2.71; N, 3.64.

Preparation of [(μ-TeCH$_2$)$_2$O]Fe$_2$(CO)$_5$(I$_{Mes}$) (12). To a stirred suspension of the imidazolium salt I$_{Mes}$·HCl (0.269 g, 0.79 mmol) in THF (20 mL) was added *t*-BuOK (0.155 g, 1.38 mmol). The mixture was stirred at room temperature for 2 h to give a yellow solution. To this solution was added complex **10** (0.094 g, 0.16 mmol), and then the new mixture was stirred at room temperature for 2 h until **10** had been completely consumed. The solvent was removed at reduced pressure, and then the residue was subjected to TLC separation using CH$_2$Cl$_2$/petroleum ether [1:4 (v/v)] as the eluent. From the main black band, **12** (0.079 g, 58%) was obtained as a black solid: mp 110−112 °C; IR (KBr disk) $\nu_{C\equiv O}$ 2016 (vs), 1949 (vs), 1901 (s) cm^{-1}; ^{1}H NMR (400 MHz, CDCl$_3$) δ 2.19 (s, 12H, 4-*o*-CH$_3$ of C$_6$H$_2$), 2.36 (s, 6H, 2-*p*-CH$_3$ of C$_6$H$_2$), 4.05−4.09 (m, 4H, CH$_2$OCH$_2$), 7.03−7.20 (m, 6H, NCH═CHN, 2C$_6$H$_2$); ^{13}C{^{1}H} NMR (100 MHz, CDCl$_3$) δ 18.8 (s, *o*-CH$_3$ of C$_6$H$_2$), 21.2 (s, *p*-CH$_3$ of C$_6$H$_2$), 44.2 (s, CH$_2$OCH$_2$), 124.7 (2s, NCH═CHN), 129.6−139.3 (m, C$_6$H$_2$), 198.9 (s, NCN), 210.8, 212.2 (2s, C≡O); ^{125}Te{^{1}H} NMR (126 MHz, CDCl$_3$, Me$_2$Te) δ −85.0. ppm. Anal. Calcd for C$_{28}$H$_{28}$Fe$_2$N$_2$O$_6$Te$_2$: C, 39.31; H, 3.30; N, 3.27. Found: C, 38.98; H, 3.27; N, 3.38.

Preparation of [(μ-TeCH$_2$)$_2$O]Fe$_2$(CO)$_5$(I$_{Me}$) (13). To a stirred suspension of the imidazolium salt I$_{Me}$·HI (0.179 g, 0.77 mmol) in THF (15 mL) was added *n*-BuLi (0.7 mL, 1.75 mmol) in a dropwise manner by a syringe to give a yellow solution. After the solution was stirred at room temperature for an additional 15 min, complex **10** (0.058 g, 0.10 mmol) was added. The new mixture was stirred at room temperature for 1 h until **10** had been completely consumed. The solvent was removed at reduced pressure, and then the residue was subjected to TLC separation using CH$_2$Cl$_2$/petroleum ether [1:2 (v/v)] as the eluent. From the main black band, **13** (0.010 g, 16%) was obtained as a black solid: mp 156−158 °C; IR (KBr disk) $\nu_{C\equiv O}$ 2011 (s), 1942 (vs), 1897 (s) cm^{-1}; ^{1}H NMR (400 MHz, CDCl$_3$) δ 3.89 (s, 6H, 2NCH$_3$), 4.46−4.58 (m, 4H, CH$_2$OCH$_2$), 6.93 (s, 2H, NCH═CHN); ^{13}C{^{1}H} NMR (100 MHz, CDCl$_3$) δ 40.5 (s, NCH$_3$), 44.8 (s, CH$_2$OCH$_2$), 123.8 (s, NCH═CHN), 182.6 (s, NCN), 213.5, 219.2 (2s, C≡O). Anal. Calcd for C$_{12}$H$_{12}$Fe$_2$N$_2$O$_6$Te$_2$: C, 22.27; H, 1.87; N, 4.33. Found: C, 22.31; H, 1.78; N, 4.12.

Electrochemical and Electrocatalytic Experiments. Acetonitrile (HPLC grade) was purchased from Amethyst Chemicals. For electrochemical and electrocatalytic experiments in MeCN, a 0.1 M solution of *n*-Bu$_4$NPF$_6$ was used as the supporting electrolyte. The *n*-Bu$_4$NPF$_6$ electrolyte was dried in an oven at 110 °C for at least 24 h. Argon was sparged through the solutions for at least 15 min before measurements were taken. The measurements were taken using a BAS Epsilon potentiostat. All voltammograms were obtained in a three-electrode cell with a 3 mm diameter glassy carbon working electrode, a platinum counter electrode, and a Ag/Ag$^+$ (0.01 M AgNO$_3$/0.1 M *n*-Bu$_4$NPF$_6$ in MeCN) reference electrode under an atmosphere of Ar. The working electrode was polished with 0.05 μm alumina paste and sonicated in water for ∼10 min. A controlled-potential electrolysis experiment was performed on a vitreous carbon rod (A = 2.9 cm^2) in a two-compartment, gastight, H-type electrolysis cell containing ∼25 mL of MeCN. All potentials are quoted against the Fc/Fc$^+$ potential. Gas chromatography was performed with a Shimadzu gas chromatograph (model GC-2014) under isothermal conditions with nitrogen as a carrier gas and a thermal conductivity detector.

Determinations of the X-ray Crystal Structures of 2, 4, 6, 7, and 10−12. While single crystals of **2**, **4**, **6**, **7**, and **10** were grown by slow evaporation of their CH$_2$Cl$_2$/*n*-hexane solutions at −10 or −5 °C, those of **11** and **12** were grown by slow diffusion of *n*-hexane into their CH$_2$Cl$_2$ solutions at room temperature. A single crystal of **2** or **4** was mounted on a Rigaku MM-007 (rotating anode) diffractometer equipped with a Saturn accessory, and their data were collected using a confocal monochromator with Mo Kα radiation (λ = 0.71070 Å) in the ω scanning mode at 113 K. A single crystal of **6** was mounted on a Rigaku MM-007 (rotating anode) diffractometer equipped with a Saturn 724 CCD accessory, and its data were collected using a multilayer monochromator with Mo Kα radiation (λ = 0.71075 Å) in the ω scanning mode at 113 K. A single crystal of **7** or **10** was mounted on a Rigaku MM-007 (rotating anode) diffractometer equipped with a Rigaku Saturn CCD accessory, and their data were collected using a confocal monochromator with Mo Kα radiation (λ = 0.71073 Å) in the ω-f scanning mode at 113 K. A single crystal of **11** or **12** was mounted on a Rigaku MM-007 (rotating anode) diffractometer equipped with a Saturn 724 CCD accessory, and its

DOI: 10.1021/acs.organomet.9b00022
Organometallics XXXX, XXX, XXX−XXX

data were collected using a multilayer monochromator with Mo Kα radiation (λ = 0.71073 Å) in the ω-f scanning mode at 113 K. Data collection, reduction, and absorption correction were performed using CRYSTALCLEAR.[57] The structures were determineed by direct methods using the SHELXS program[58] and refined by full-matrix least-squares techniques (SHELXL)[59] on F^2. Hydrogen atoms were located by using the geometric method. Details of crystal data, data collections, and structural refinements are summarized in Tables 4−6.

■ ASSOCIATED CONTENT

Supporting Information

The Supporting Information is available free of charge on the ACS Publications website at DOI: 10.1021/acs.organomet.9b00022.

Synthesis and characterization of **X**−**Z** and **D**−**F**, ORTEP views of **Z** and **F** (Figures S1 and S2, respectively), crystal data and structural refinement details of **Z** and **F** (Table S1), ^{13}C−^{1}H HMQC and HMBC spectra of complexes **7**−**9**, and some electrochemical and electrocatalytic data and plots (Figures S9−S11) (PDF)

Accession Codes

CCDC 1852760−1852768 contain the supplementary crystallographic data for this paper. These data can be obtained free of charge via www.ccdc.cam.ac.uk/data_request/cif, or by emailing data_request@ccdc.cam.ac.uk, or by contacting The Cambridge Crystallographic Data Centre, 12 Union Road, Cambridge CB2 1EZ, UK; fax: +44 1223 336033.

■ AUTHOR INFORMATION

Corresponding Author

*E-mail: lcsong@nankai.edu.cn.

ORCID

Li-Cheng Song: 0000-0003-0964-8869

Notes

The authors declare no competing financial interest.

■ ACKNOWLEDGMENTS

The authors are grateful to the National Natural Science Foundation of China (21772106) and Technology of China (973 program 2014CB845604) for financial support.

■ REFERENCES

(1) For reviews, see for example: (a) Song, L.-C. Synthesis of Butterfly-Shaped Fe/E (E = S, Se, Te) Cluster Complexes from in situ Reactions of Novel Organometallic Anions of Type $[(\mu\text{-RE})(\mu\text{-CO})Fe_2(CO)_6]^-$ (E = S, Se, Te). *Trends Organomet. Chem.* **1999**, *3*, 1−20. (b) Song, L.-C. Recent studies on chemistry of novel μ-CO-containing butterfly Fe/E (E = S, Se, Te) cluster salts. *Sci. China, Ser. B: Chem.* **2009**, *52*, 1−14. (c) Song, L.-C. Investigations on Butterfly Fe/S Cluster S-Centered Anions $(\mu\text{-S}^-)_2Fe_2(CO)_6(\mu\text{-S}^-)(\mu\text{-RS})\text{-}Fe_2(CO)_6$ and Related Species. *Acc. Chem. Res.* **2005**, *38*, 21−28. (d) Li, Y.; Rauchfuss, T. B. Synthesis of Diiron(I) Dithiolato Carbonyl Complexes. *Chem. Rev.* **2016**, *116*, 7043−7077.

(2) Seyferth, D.; Henderson, R. S.; Song, L.-C. The dithiobis(tricarbonyliron) dianion: Improved preparation and new chemistry. *J. Organomet. Chem.* **1980**, *192*, C1−C5.

(3) Seyferth, D.; Song, L.-C.; Henderson, R. S. Novel Boron-to-Sulfur Alkyl Group Transfer in Reactions of Lithium Triethylborohydride-Derived Bis(μ-thiolato)-bis(tricarbonyliron) Dianion with Mercuric Chloride and Alkylmercuric Chlorides. *J. Am. Chem. Soc.* **1981**, *103*, 5103−5107.

(4) Winter, A.; Zsolnai, L.; Huttner, G. Dinuclear and Trinuclear Carbonyliron Complexes Containing 1,2- and 1,3-Dithiolato Bridging Ligands. *Z. Z. Naturforsch., B: J. Chem. Sci.* **1982**, *37b*, 1430−1436.

(5) Bose, K. S.; Sinn, E.; Averill, B. A. Synthesis and X-ray Structure of the $[Fe_4S_4(CO)_{12}]^{2-}$ Ion: An Example of Intermolecular Disulfide Formation by the $(\mu\text{-S})_2Fe_2(CO)_6$ Unit. *Organometallics* **1984**, *3*, 1126−1128.

(6) Kovacs, J. A.; Bashkin, J. K.; Holm, R. H. Persulfide-Bridged Iron-Molybdenum-Sulfur Clusters of Biological Relevance: Two Synthetic Routes and the Structures of Intermediate and Product Clusters. *J. Am. Chem. Soc.* **1985**, *107*, 1784−1786.

(7) Mathur, P.; Reddy, V. D. Reduction of $(\mu_2\text{-Te}_2)Fe_2(CO)_6$ and reaction of the dianion formed with metal dihalides, L_2MCl_2(L = PPh_3M = Pt, Pd, Ni; L = C_5H_5M = Ti; L = Me, n-Bu, M = Sn). *J. Organomet. Chem.* **1990**, *385*, 363−368.

(8) Song, L.-C.; Fan, H.-T.; Hu, Q.-M. The First Example of Macrocycles Containing Butterfly Transition Metal Cluster Cores via Novel Tandem Reactions. *J. Am. Chem. Soc.* **2002**, *124*, 4566−4567.

(9) (a) Cammack, R. Hydrogenase sophistication. *Nature* **1999**, *397*, 214−215. (b) Adams, M. W. W.; Stiefel, E. I. Biological Hydrogen Production: Not So Elementary. *Science* **1998**, *282*, 1842−1843.

(10) Peters, J. W.; Lanzilotta, W. N.; Lemon, B. J.; Seefeldt, L. C. X-ray Crystal Structure of the Fe-Only Hydrogenase (CpI) from *Clostridium pasteurianum* to 1.8 Angstrom Resolution. *Science* **1998**, *282*, 1853−1858.

(11) Nicolet, Y.; Piras, C.; Legrand, P.; Hatchikian, E. C.; Fontecilla-Camps, J. C. *Desulfovibrio desulfuricans* iron hydrogenase: the structure shows unusual coordination to an active site Fe binuclear center. *Structure* **1999**, *7*, 13−23.

(12) Nicolet, Y.; De Lacey, A. L.; Vernède, X.; Fernandez, V. M.; Hatchikian, E. C.; Fontecilla-Camps, J. C. Crystallographic and FTIR Spectroscopic Evidence of Changes in Fe Coordination Upon Reduction of the Active Site of the Fe-Only Hydrogenase from *Desulfovibrio desulfuricans*. *J. Am. Chem. Soc.* **2001**, *123*, 1596−1601.

(13) Pierik, A. J.; Hulstein, M.; Hagen, W. R.; Albracht, S. P. J. A low-spin iron with CN and CO as intrinsic ligands forms the core of the active site in [Fe]-hydrogenases. *Eur. J. Biochem.* **1998**, *258*, 572−578.

(14) De Lacey, A. L.; Stadler, C.; Cavazza, C.; Hatchikian, E. C.; Fernandez, V. M. FTIR Characterization of the Active Site of the Fe-hydrogenase from *Desulfovibrio desulfuricans*. *J. Am. Chem. Soc.* **2000**, *122*, 11232−11233.

(15) Chen, Z.; Lemon, B. J.; Huang, S.; Swartz, D. J.; Peters, J. W.; Bagley, K. A. Infrared Studies of the CO-Inhibited Form of the Fe-Only Hydrogenase from *Clostridium pasteurianum* I: Examination of Its Light Sensitivity at Cryogenic Temperatures. *Biochemistry* **2002**, *41*, 2036−2043.

(16) Silakov, A.; Wenk, B.; Reijerse, E.; Lubitz, W. ^{14}N HYSCORE investigation of the H-cluster of [FeFe] hydrogenase: evidence for a nitrogen in the dithiol bridge. *Phys. Chem. Chem. Phys.* **2009**, *11*, 6592−6599.

(17) Berggren, G.; Adamska, A.; Lambertz, C.; Simmons, T. R.; Esselborn, J.; Atta, M.; Gambarelli, S.; Mouesca, J.-M.; Reijerse, E.; Lubitz, W.; Happe, T.; Artero, V.; Fontecave, M. Biomimetic assembly and activation of [FeFe]-hydrogenases. *Nature* **2013**, *499*, 66−69.

(18) Adams, M. W. W. The structure and mechanism of iron-hydrogenases. *Biochim. Biophys. Acta, Bioenerg.* **1990**, *1020*, 115−145.

(19) For reviews, see for example: (a) Tard, C.; Pickett, C. J. Structural and Functional Analogues of the Active Sites of the [Fe]-, [NiFe]-, and [FeFe]-Hydrogenases. *Chem. Rev.* **2009**, *109*, 2245−2274. (b) Lubitz, W.; Ogata, H.; Rüdiger, O.; Reijerse, E. Hydrogenases. *Chem. Rev.* **2014**, *114*, 4081−4148. (c) Simmons, T. R.; Berggren, G.; Bacchi, M.; Fontecave, M.; Artero, V. Mimicking hydrogenases: From biomimetics to artificial enzymes. *Coord. Chem. Rev.* **2014**, *270*−*271*, 127−150. (d) Schilter, D.; Camara, J. M.; Huynh, M. T.; Hammes-Schiffer, S.; Rauchfuss, T. B. Hydrogenase Enzymes and Their Synthetic Models: The Role of Metal Hydrides. *Chem. Rev.* **2016**, *116*, 8693−8749. (e) Harb, M. K.; Apfel, U.-P.;

DOI: 10.1021/acs.organomet.9b00022
Organometallics XXXX, XXX, XXX−XXX

Sakamoto, T.; El-Khateeb, M.; Weigand, W. Diiron Dichalcogenolato (Se and Te) Complexes: Models for the Active Site of [FeFe] Hydrogenase. *Eur. J. Inorg. Chem.* **2011**, *2011*, 986−993.

(20) Justice, A. K.; Rauchfuss, T. B.; Wilson, S. R. Unsaturated, Mixed-Valence Diiron Dithiolate Model for the H_{ox} State of the [FeFe] Hydrogenase. *Angew. Chem., Int. Ed.* **2007**, *46*, 6152−6153.

(21) Lunsford, A. M.; Beto, C. C.; Ding, S.; Erdem, Ö. F.; Wang, N.; Bhuvanesh, N.; Hall, M. B.; Darensbourg, M. Y. Cyanide-bridged iron complexes as biomimetics of tri-iron arrangements in maturases of the H cluster of the di-iron hydrogenase. *Chem. Sci.* **2016**, *7*, 3710−3719.

(22) Razavet, M.; Davies, S. C.; Hughes, D. L.; Barclay, J. E.; Evans, D. J.; Fairhurst, S. A.; Liu, X.; Pickett, C. J. All-iron hydrogenase: synthesis, structure and properties of {2Fe3S}-assemblies related to the di-iron sub-site of the H-cluster. *Dalton Trans.* **2003**, 586−595.

(23) Capon, J.-F.; El Hassnaoui, S.; Gloaguen, F.; Schollhammer, P.; Talarmin, J. N-Heterocyclic Carbene Ligands as Cyanide Mimics in Diiron Models of the All-Iron Hydrogenase Active Site. *Organometallics* **2005**, *24*, 2020−2022.

(24) Liu, T.; Darensbourg, M. Y. A Mixed-Valent, Fe(II)Fe(I), Diiron Complex Reproduces the Unique Rotated State of the [FeFe]Hydrogenase Active Site. *J. Am. Chem. Soc.* **2007**, *129*, 7008−7009.

(25) Ghosh, S.; Hogarth, G.; Hollingsworth, N.; Holt, K. B.; Richards, I.; Richmond, M. G.; Sanchez, B. E.; Unwin, D. Models of the iron-only hydrogenase: a comparison of chelate and bridge isomers of $Fe_2(CO)_4\{Ph_2PN(R)PPh_2\}(\mu\text{-pdt})$ as proton-reduction catalysts. *Dalton Trans.* **2013**, *42*, 6775−6792.

(26) Heinekey, D. M. Hydrogenase enzymes: Recent structural studies and active site models. *J. Organomet. Chem.* **2009**, *694*, 2671−2680.

(27) Kluwer, A. M.; Kapre, R.; Hartl, F.; Lutz, M.; Spek, A. L.; Brouwer, A. M.; van Leeuwen, P. W. N. M.; Reek, J. N. H. Self-assembled biomimetic [2Fe2S]-hydrogenase-based photocatalyst for molecular hydrogen evolution. *Proc. Natl. Acad. Sci. U. S. A.* **2009**, *106*, 10460−10465.

(28) Song, L.-C.; Yang, Z.-Y.; Bian, H.-Z.; Liu, Y.; Wang, H.-T.; Liu, X.-F.; Hu, Q.-M. Diiron Oxadithiolate Type Models for the Active Site of Iron-Only Hydrogenases and Biomimetic Hydrogen Evolution Catalyzed by $Fe_2(\mu\text{-}SCH_2OCH_2S\text{-}\mu)(CO)_6$. *Organometallics* **2005**, *24*, 6126−6135.

(29) Song, L.-C.; Tang, M.-Y.; Su, F.-H.; Hu, Q.-M. A Biomimetic Model for the Active Site of Iron-Only Hydrogenases Covalently Bonded to a Porphyrin Photosensitizer. *Angew. Chem., Int. Ed.* **2006**, *45*, 1130−1133.

(30) Song, L.-C.; Wang, Y.-X.; Xing, X.-K.; Ding, S.-D.; Zhang, L.-D.; Wang, X.-Y.; Zhang, H.-T. Hydrophilic Quaternary Ammonium-Group-Containing [FeFe]-Hydrogenase Models: Synthesis, Structures, and Electrocatalytic Hydrogen Production. *Chem. - Eur. J.* **2016**, *22*, 16304−16314.

(31) (a) Song, L.-C.; Gao, W.; Feng, C.-P.; Wang, D.-F.; Hu, Q.-M. Investigations on Synthesis, Structure, and Properties of New Butterfly [2Fe2Se] Cluster Complexes Relevant to Active Sites of Some Hydrogenases. *Organometallics* **2009**, *28*, 6121−6130. (b) Song, L.-C.; Gai, B.; Feng, Z.-H.; Du, Z.-Q.; Xie, Z.-J.; Sun, X.-J.; Song, H.-B. Synthesis, Structures, and Some Properties of Diiron Oxadiselenolate (ODSe) and Thiodiselenolate (TDSe) Complexes as Models for the Active Site of [FeFe]-Hydrogenases. *Organometallics* **2013**, *32*, 3673−3684.

(32) Kertess, L.; Wittkamp, F.; Sommer, C.; Esselborn, J.; Rüdiger, O.; Reijerse, E. J.; Hofmann, E.; Lubitz, W.; Winkler, M.; Happe, T.; Apfel, U.-P. Chalcogenide substitution in the [2Fe] cluster of [FeFe]-hydrogenases conserves high enzymatic activity. *Dalton Trans.* **2017**, *46*, 16947−16958.

(33) Gao, W.; Song, L.-C.; Yin, B.-S.; Zan, H.-N.; Wang, D.-F.; Song, H.-B. Synthesis and Characterization of Single, Double, and Triple Butterfly [2Fe2E] (E = Se, S) Cluster Complexes Related to the Active Site of [FeFe]-Hydrogenases. *Organometallics* **2011**, *30*, 4097−4107.

(34) Harb, M. K.; Niksch, T.; Windhager, J.; Görls, H.; Holze, R.; Lockett, L. T.; Okumura, N.; Evans, D. H.; Glass, R. S.; Lichtenberger, D. L.; El-Khateeb, M.; Weigand, W. Synthesis and Characterization of Diiron Diselenolato Complexes Including Iron Hydrogenase Models. *Organometallics* **2009**, *28*, 1039−1048.

(35) Apfel, U.-P.; Halpin, Y.; Gottschaldt, M.; Görls, H.; Vos, J. G.; Weigand, W. Functionalized Sugars as Ligands towards Water-Soluble [Fe-only] Hydrogenase Models. *Eur. J. Inorg. Chem.* **2008**, *2008*, 5112−5118.

(36) Harb, M. K.; Apfel, U.-P.; Kübel, J.; Görls, H.; Felton, G. A. N.; Sakamoto, T.; Evans, D. H.; Glass, R. S.; Lichtenberger, D. L.; El-Khateeb, M.; Weigand, W. Preparation and Characterization of Homologous Diiron Dithiolato, Diselenato, and Ditellurato Complexes: [FeFe]-Hydrogenase Models. *Organometallics* **2009**, *28*, 6666−6675.

(37) Song, L.-C.; Li, Q.-L.; Feng, Z.-H.; Sun, X.-J.; Xie, Z.-J.; Song, H.-B. Synthesis, characterization, and electrochemical properties of diiron propaneditellurolate (PDTe) complexes as active site models of [FeFe]-hydrogenases. *Dalton Trans.* **2013**, *42*, 1612−1626.

(38) Herrmann, W. A.; Schütz, J.; Frey, G. D.; Herdtweck, E. *N*-Heterocyclic Carbenes: Synthesis, Structures, and Electronic Ligand Properties. *Organometallics* **2006**, *25*, 2437−2448.

(39) Mercs, L.; Labat, G.; Neels, A.; Ehlers, A.; Albrecht, M. Piano-Stool Iron(II) Complexes as Probes for the Bonding of *N*-Heterocyclic Carbenes: Indications for π-Acceptor Ability. *Organometallics* **2006**, *25*, 5648−5656.

(40) Viciano, M.; Mas-Marzá, E.; Sanaú, M.; Peris, E. Synthesis and Reactivity of New Complexes of Rhodium and Iridium with Bis(dichloroimidazolylidene) Ligands. Electronic and Catalytic Implications of the Introduction of the Chloro Substituents in the NHC Rings. *Organometallics* **2006**, *25*, 3063−3069.

(41) Arduengo, A. J., III; Dias, H. V. R.; Harlow, R. L.; Kline, M. Electronic Stabilization of Nucleophilic Carbenes. *J. Am. Chem. Soc.* **1992**, *114*, 5530−5534.

(42) Buchgraber, P.; Toupet, L.; Guerchais, V. Syntheses, Properties, and X-ray Crystal Structures of Piano-Stool Iron Complexes Bearing an N-Heterocyclic Carbene Ligand. *Organometallics* **2003**, *22*, 5144−5147.

(43) Takikawa, Y.; Koyama, Y.; Yoshida, T.; Makino, K.; Shibuya, H.; Sato, K.; Otsuka, T.; Shibata, Y.; Onuma, Y.; Aoyagi, S.; Shimada, K.; Kabuto, C. Synthesis and Oxidative Ring Contraction of 1,5,3,7-Dichalcogenadiazocanes. Novel Formation of 1,2,4-Diselenazolidines, 1,2,4-Ditellurazolidines, and 1,2,3,4,5,7-Pentathiazocanes. *Bull. Chem. Soc. Jpn.* **2006**, *79*, 1913−1925.

(44) Seyferth, D.; Womack, G. B.; Song, L.-C.; Cowie, M.; Hames, B. W. Unexpected Intramolecular Nucleophilic Substitution in an Anionic $Fe_2(CO)_6$ Complex with an Organosulfur Ligand. A Novel Preparation of $Fe_2(CO)_6$ Complexes of Dithioformic Acid Esters. *Organometallics* **1983**, *2*, 928−930.

(45) Song, L.-C.; Mei, S.-Z.; Feng, C.-P.; Gong, F.-H.; Ge, J.-H.; Hu, Q.-M. Reactions of Monoanions $[(\mu\text{-RE})(\mu\text{-E})Fe_2(CO)_6]^-$ and Dianions $[(\mu\text{-E})_2Fe_2(CO)_6]^{2-}$ (E = Se, S) with N-Substituted Benzimidoyl Chlorides, Leading to Novel Butterfly Fe/E Cluster Complexes. *Organometallics* **2010**, *29*, 5050−5056.

(46) Song, L.-C.; Yan, C.-G.; Hu, Q.-M.; Wang, R.-J.; Mak, T. C. W.; Huang, X.-Y. Formation of $(\mu\text{-RE})(\mu\text{-S}^-)Fe_2(CO)_6$ and $(\mu\text{-RE})(\mu\text{-Se}^-)Fe_2(CO)_6$ (E = S, Se) Anions and a Comparative Study of Their Reactions with $SO_2Cl_2ClC(O)ZC(O)Cl$ (Z = $(CH_2)_2C_6H_4$), or *p*-$MeC_6H_4SO_2Cl$. Single-Crystal Structures of $[(\mu\text{-EtS})Fe_2(CO)_6]_2(\mu_4\text{-Se})$ and $(\mu\text{-EtS})(\mu\text{-}p\text{-}MeC_6H_4SO_2)Fe_2(CO)_6$. *Organometallics* **1996**, *15*, 1535−1544.

(47) Collman, J. P.; Hegedus, L. S. *Principles and Applications of Organotransition Metal Chemistry*; University Science Books: Mill Valley, CA, 1980; pp 54−88.

(48) Bard, A. J.; Faulkner, L. R. *Electrochemical Methods: Fundamentals and Applications*, 2nd ed.; John Wiley & Sons: Hoboken, NJ, 2001.

(49) Abul-Futouh, H.; Skabeev, A.; Botteri, D.; Zagranyarski, Y.; Görls, H.; Weigand, W.; Peneva, K. Toward a Tunable Synthetic

DOI: 10.1021/acs.organomet.9b00022
Organometallics XXXX, XXX, XXX−XXX

[FeFe]-Hydrogenase H-Cluster Mimic Mediated by Perylene Monoimide Model Complexes: Insight into Molecular Structures and Electrochemical Characteristics. *Organometallics* **2018**, *37*, 3278−3285.

(50) Felton, G. A. N.; Glass, R. S.; Lichtenberger, D. L.; Evans, D. H. Iron-Only Hydrogenase Mimics. Thermodynamic Aspects of the Use of Electrochemistry to Evaluate Catalytic Efficiency for Hydrogen Generation. *Inorg. Chem.* **2006**, *45*, 9181−9184.

(51) King, R. B. *Organometallic Syntheses, Transition-Metal Compounds*; Academic Press: New York, 1965; Vol. *1*, pp 95.

(52) Arduengo, A. J., III; Krafczyk, R.; Schmutzler, R.; Craig, H. A.; Goerlich, J. R.; Marshall, W. J.; Unverzagt, M. Imidazolylidenes, Imidazolinylidenes and Imidazolidines. *Tetrahedron* **1999**, *55*, 14523−14534.

(53) Oertel, A. M.; Ritleng, V.; Burr, L.; Chetcuti, M. J. Synthesis and Structural Characterization of Half-Sandwich Nickel Complexes Bearing Two Different N-Heterocyclic Carbene Ligands. *Organometallics* **2011**, *30*, 6685−6691.

(54) Lee, H. M.; Lu, C. Y.; Chen, C. Y.; Chen, W. L.; Lin, H. C.; Chiu, P. L.; Cheng, P. Y. Palladium complexes with ethylene-bridged bis(*N*-heterocyclic carbene) for C-C coupling reactions. *Tetrahedron* **2004**, *60*, 5807−5825.

(55) Song, L.-C.; Li, C.-G.; Gao, J.; Yin, B.-S.; Luo, X.; Zhang, X.-G.; Bao, H.-L.; Hu, Q.-M. Synthesis, Structure, and Electrocatalysis of Diiron C-Functionalized Propanedithiolate (PDT) Complexes Related to the Active Site of [FeFe]-Hydrogenases. *Inorg. Chem.* **2008**, *47*, 4545−4553.

(56) Lesch, D. A.; Rauchfuss, T. B. Isolation and Characterization of $Fe_2(\mu\text{-}Te_2)(CO)_6$ and Its Conversion to $Fe_3(\mu_3\text{-}Te)_2(CO)_x$ (x = 9, 10). *Inorg. Chem.* **1981**, *20*, 3583−3585.

(57) *CrystalClear and CrystalStructure*; Rigaku and Rigaku Americas: The Woodlands, TX, 2007.

(58) (a) Sheldrick, G. M. *SHELXS97 and SHELXL-97, Program for Crystal Structure Solution and Refinement*; University of Göttingen: Göttingen, Germany, 1997. (b) Sheldrick, G. M. A short history of *SHELX. Acta Crystallogr., Sect. A: Found. Crystallogr.* **2008**, *64*, 112−122.

(59) Sheldrick, G. M. *SHELXT*-Integrated space-group and crystalstructure determination. *Acta Crystallogr., Sect. A: Found. Adv.* **2015**, *71*, 3−8.

DOI: 10.1021/acs.organomet.9b00022
Organometallics XXXX, XXX, XXX−XXX